AD_____

AWARD NUMBER: W81XWH-11-1-0327

TITLE: Inhibition of Embryonic Genes to Control Colorectal Cancer Metastasis

PRINCIPAL INVESTIGATOR: John Milburn Jessup, MD

RECIPIENT: Geneva Foundation

Lakewood, WA 98499-3976

REPORT DATE: September 2014

TYPE OF REPORT: Annual

PREPARED FOR: U.S. Army Medical Research and Materiel Command
Fort Detrick, Maryland 21702-5012

REPORT DOCUMENTATION PAGE

Form Approved
OMB No. 0704-0188

1. REPORT DATE	2. REPORT TYPE Annual	3. DATES COVERED
September 2014		1 Sep 2013 - 31 Aug 2014

4. TITLE AND SUBTITLE
Inhibition of Embryonic Genes to Control Colorectal Cancer Metastasis

5a. CONTRACT NUMBER
W81XWH-11-1-0327

5b. GRANT NUMBER

5c. PROGRAM ELEMENT NUMBER

6. AUTHOR(S)
John Milburn Jessup, MD

E-Mail: jessupj@mail.nih.gov

5d. PROJECT NUMBER

5e. TASK NUMBER

5f. WORK UNIT NUMBER

7. PERFORMING ORGANIZATION NAME(S) AND ADDRESS(ES)

Geneva Foundation
Lakewood, WA 98499-3976

8. PERFORMING ORGANIZATION REPORT NUMBER

9. SPONSORING / MONITORING AGENCY NAME(S) AND ADDRESS(ES)

U.S. Army Medical Research and Materiel Command
Fort Detrick, Maryland 21702-5012

10. SPONSOR/MONITOR'S ACRONYM(S)

11. SPONSOR/MONITOR'S REPORT NUMBER(S)

12. DISTRIBUTION / AVAILABILITY STATEMENT

Approved for Public Release; Distribution Unlimited

13. SUPPLEMENTARY NOTES
The views, opinions and/or finding contained in this report are those of the authors(s) and should not be construed as an official Department of the Army position, policy unless so designated by other documentation.

14. ABSTRACT

Embryonic core transcription factors (TFs), primarily the retrogene NanogP8, are the master regulators of cancer stem cells (CSC) in human colorectal carcinoma (CRC). The corollary is that inhibition of NanogP8 will inhibit neoplastic progression of CRC. During the second year of funding we confirmed that NANOG is expressed in the majority of primary human colon carcinomas and that its expression is a significant prognostic factor, especially when associated with expression of the cell adhesion scaffold protein NEDD9. We also elucidated that inhibition of NANOGP8 and/or NANOG induces apoptosis through inhibition of MCL-1 as well as proof of the principle that vector-delivered shRNA to NANOGP8 and/or NANOG complements inhibition of BCL-2 and BCL-XL as a means to inhibit and kill human colorectal cells. Finally we have demonstrated that intralesional injection of LV-delivered shRNA to NANOGP8 or NANOG transduces tumor cells within xenografts growing in vivo in NOD/SCID mice as well as the probable need to create a conditionally replicating adenovirus

15. SUBJECT TERMS
Nothing Listed

16. SECURITY CLASSIFICATION OF:			17. LIMITATION OF ABSTRACT	18. NUMBER OF PAGES	19a. NAME OF RESPONSIBLE PERSON
a. REPORT	b. ABSTRACT	c. THIS PAGE			USAMRMC
U	U	U	UU	81	19b. TELEPHONE NUMBER *(include area code)*

Standard Form 298 (Rev. 8-98)
Prescribed by ANSI Std. Z39.18

Table of Contents

Annual Report – Third Year of Funding

Hypothesis: Embryonic core transcription factors (TFs), primarily the retrogene NanogP8, are the master regulators of cancer stem cells (CSC) in human colorectal carcinoma (CRC). The corollary is that inhibition of NanogP8 will inhibit neoplastic progression of CRC.

Introduction

During the first two years of funding we completed two of the three Tasks and identified new information that establishes the importance of the NANOGs, including NANOGP8, in maintaining the stemness of colorectal carcinoma (CRC) as well as the identification of two different pathways by which NANOG and NANOGP8 control pluripotency in CRC. We have described how we established the importance of NANOGP8 in the maintenance of the stem cell characteristics of CRC and then what we have done to meet the specific aims.

Original Tasks and Associated Milestones from SOW:

1) **Confirm that *NANOGP8* is the dominant Nanog family member expressed in human CRC**

1a. Measure Nanog gene product expression in primary CRC by quantitative immunofluorescence assay (qIFA). Completed with 75% of Colon Carcinomas primaries expressing a NANOG protein. This was a negative prognostic factor, especially when protein expression was combined with a NANOG regulated scaffolding factor NADD9.

1b. Identify the relative transcript expression of Nanog, NanogP8, other family members in CRC by quantitative Reverse Transcriptase-Polymerase Chain reaction (qRT-PCR) and RE Assay. Completed with ~80% of CRC metastases expressing a *NANOG* transcript with two-thirds being *NANOGP8* and 5% each being *NANOGP4* and *NANOGP7*. In one-third NANOG was the only transcript and in one-third *NANOGP8* was the only transcript detected. Often there was more than *NANOG* family transcript expressed. In silico analysis of the *NANOG* and *NANOGP8* promoters demonstrate only 40% homology but consensus binding sites for 9 common transcription factors are present in both promoters.

2) **Determine whether inhibition of *NANOG, SOX2*, or *OCT4* by lentiviral vector shRNA causes apoptosis and inhibition of cell proliferation in CRC.**

2a. Determine whether inhibition of NanogP8 or other embryonic TFs by LV shRNA inhibits cell proliferation in CRC in vitro Completed. We showed that proliferation was inhibited in 3 CRC lines in monolayer culture. shRNA to *NANOGP8* was more effective than shRNA to *NANOG*. Also inhibition of *NANOGs* inhibited the other transcription factors. shRNA to OCT4 and SOX2 was not as effective in inhibiting proliferation.

2b. Establish whether transduction of shRNA targeting NanogP8 induces apoptosis in CRC lines. Completed. shRNA to NANOGP8 induces minimal apoptosis in monolayer culture when all *NANOG* transcript levels are low. However, inhibition of the *NANOGs* in suspension culture when the number of total *NANOG* transcripts increases causes apoptosis through the intrinsic pathway involving the activation of Caspase 9 and Caspase 3. This is in distinction to the mechanism of cell death termed anoikis that is a form of apoptosis caused in suspension culture that utilizes the extrinsic pathway in CRC. *Manuscript is under review*. The MOI to cause 50% inhibition of growth is between 5 and 10 for shRNA to *NANOGP8* and this causes at least a 50% inhibition of growth in 3-D suspension and monolayer cultures.

The third year was focused on the completion of the third task or aim. As reported last year, we have had tremendous difficulty in achieving transduction after intra-tumoral injection. We achieved less than 1% transduction efficiency after injecting 10^8-10^{10} viral particles into 3 mm subcutaneous lesions. This led us to hire Dr. Nikolay Korokhov to produce lentivirus as well as to develop an alternative approach for gene therapy that is within the scope of this project. Dr. Korokhov has long experience with production of both lentivirus and adenovirus and was in charge of production at VIRxSYS, the company that went out of business as this project started but was supposed to be the provider of third generation lentivirus that was similar to what they were using in clinical trials. Dr. Korokhov was laid off and able to work with us. His resume was attached in last year's report that also gave our plan to develop oncolytic adenoviruses as an alternative to the lentivirus as a vector for our shRNAs.

This report details our testing an improved preparation of lentivirus in vivo, its shortcomings and the ability of oncolytic adenovirus to inhibit human colorectal xenografts.

Keywords

LV – Lentivirus
CRC- colorectal carcinoma
CSC- cancer stem cell(s)
shRNA – short hairpin RNA
NANOG, NANOGP8, , SOX2 – gene names
SOW- statement of work
Ad5/3- chimeric adenovirus with a type 5 fiber and type 3 knob
CRAd- Conditionally replicating adenovirus
3T3- normal immortal mouse fibroblast cell line

Accomplishments

During the third year of this project we focused first on lentivrus as a vector for shRNA and its shortcomings. This is to complete Task 3 from the SOW:

3) **Determine the efficacy of treatment with local or systemic lentiviral shRNA targeting NanogP8 or other embryonic genes on regression of established human CRC metastases in the livers of NOD/SCID mice**

3a. Determine the efficacy of intralesional injection of lentivirus shRNA to NanogP8 or other embryonic genes on CRC tumors in the livers of NOD/SCID mice. Partially Completed. As previously reported in prior annual reports, we had tremendous difficulty with transducing human CRC cells in subcutaneous nodules. At MOI of 5 -10 or higher we did not achieve a transduction rate that was even 1% of total tumor cells using LV shRNAs. We finally were able to hire Dr. Korokhov who was a quality control and production manager for VIRxSYS that company that was to produce third generation LV shRNA for us. Thankfully, Dr. Korokhov was able to assist us with preparation of lentivirus for in vivo injection. He purified lentivirus for use in vivo by column filtration and high-speed centrifugaton. He indicated that the presence of serum components from tissue culture medium often inhibited transduction and was the likely cause of the inefficient transduction in vivo as well as the difference caused by host stroma.

We finally had enough purified lentivirus to achieve a 5 MOI for intratumoral injection of 3-6 mm diameter subcutaneous nodules of CX-1 in NOD/SCID mice treated 9 days after injection of 3 x 10^6 viable cells. Lentivirus (LV) shNEG is the negative control along with mice that were not injected. The LV shNEG control demonstrates that intratumoral injection by itself does not inhibit CX-1 tumor growth. As can be seen in Figure 1A, the single injection of LV with shRNA to *NANOG* (LV shNG-1) or *NANOGP8* (LV shNp8-1) inhibited growth of CX-1 (Figure 1A). Assessment of tumors 3 days after lentiviral injection demonstrated that viral transduction occurred in ~20% of CX-1 cells (data not shown). As can be seen in Figure 1A, growth of CX-1 was inhibited for 11 days after intratumoral injection. This proves that lentiviral shRNA to *NANOG/NANOGP8* is able to inhibit growth of human colorectal carcinoma – at least after one injection. Unfortunately, the non-transduced CX-1 cells grew out after 11 days and quickly reversed the inhibition of tumor growth as indicated by the nonsignificant difference in both the area and the weights of the tumors in the four treatment groups (Figure 1B).

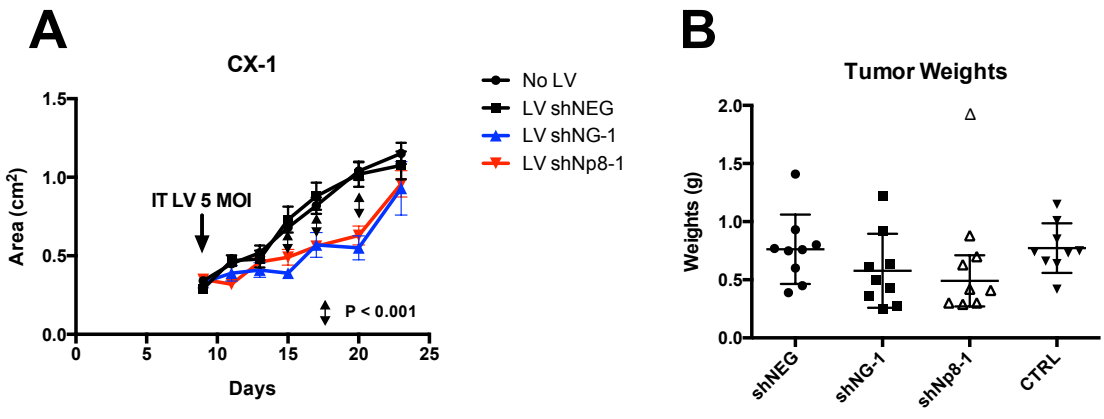

Figure 1. Lentiviral Allele-Specific shRNAs to *NANOG or NANOGP8* inhibit Growth of CX-1 Subcutaneous Nodules. ***Panel A:*** *Three million viable CX-1 cells were injected into groups of 10 six week old NOD/SCID males and then 9 days later were treated with lentiviral (LV) shRNA as indicated intra-tumorally at MOI of 5. (shNEG is a control shRNA, shNG-1 is shRNA that inhibits NANOG, and shNp8-1 inhibits NANOGP8). Results are area (product of 2 largest perpendicular diameters) expressed as mean ± SEM. P values determined by one way ANOVA with Tukey test of means corrected for multiple comparisons.* ***Panel B****: Tumor weights when mice euthanized on day 24 after tumor inoculation. There is a trend toward lighter tumors in the shNp8-1 and shNG-1 groups but it is not significant by one way ANOVA.*

This supports the ability of an shRNA to inhibit growth *in vivo*. However, lentivirus is a non-replicating virus and 4 days after the last measurement it was apparent that tumors were growing because when mice were sacrificed, the

weights of tumor in all groups were not significantly different (Figure 1B). This indicates that while shRNA effectively inhibits the growth of those cells in which it is expressed by stable integration by the lentivirus, eventually tumor cells that are not transduced will grow and lead to progressive tumor growth. This is why a replicating oncolytic virus is important because it may continue to infect and kill cancer cells either through direct lysis or through the effects of the shRNA or other genetic payload.

Since the LV shRNA construct did not cause long lasting inhibition of subcutaneous xenograft growth, Tasks 3b and 3c were not completed because they depended on the ability of LVshRNA to achieve inhibition of tumor growth for at least 21 days after intra-tumoral injection. The inability to achieve this goal in a human CRC cell line that is sensitive to LVshRNA to *NANOG* and *NANOGP8* indicates that lentivirus is not likely to be a good vector for gene therapy even though the payload was transiently effective in inhibiting cell growth. In addition, lentivirus is not an effective viral vector because it is relatively expensive to prepare and requires fairly extensive clean up through column filtration and centrifugation.

Impact

This project has shown that intratumoral Lentiviral delivery of shRNA to tumor masses is not likely to control tumor growth for longer than a week. This is important and justifies the development of the oncolytic viruses that are described in the next section.

Other Impact is that we have demonstrated that inhibition of *NANOG* and *NANOGP8* decrease the expression of MCL1 that increases the efficacy of BH3 peptidomimetic inhibitors that cause apoptosis in cancer cells. Thus, inhibition of the *NANOGs* may support the concept that *NANOG* and its family members are master regulators of stemness.

Change/Problems

Justification For Also Developing A Conditional Replicating Adenoviral (CRAd) Vector

As we described last year, a MOI of at least 5 but more likely 10 viral particles to each tumor cell is necessary. Since a 1 cm tumor contains 10^9 cells and most tumors are on average 2 cm at diagnosis, then one needs ~10^{10} viral particles to deliver enough shRNA to infect and transduce a 1-2 cm tumor in a patient. Patients with multiple metastases would need $10^{11\text{-}12}$ viral particles for treatment. Since large scale preparation of lentivirus generally yields ~10^{10} infectious particles total per run, it is not likely that a non-replicating vector will be able to inhibit the growth of cancers in patients with more than minimal disease that may be controlled by standard current therapies easily. I did not appreciate these facts when submitting the application and have learned them during the course of our work.

The solution to this problem is to create a vector that can selectively replicate within a cancer but not in normal tissue. There is a replicating lentivector that was originally described in the early 2000's, but this vector depends on the administration of doxycycline and has a potential for recombination to recreate wild type HIV. However, this potential to revert to a replicating HIV along with the fact that it cannot be easily pseudotyped to not infect immune cells make this conditional replicating virus of limited usefulness. We have been in contact with the developer of this vector, Prof. Berkhout in the Netherlands, but further modification of this vector is not an option because the lentiviral genome is highly complex with multiple genes interlaced within a stretch of viral genome RNA and with controls that still are not well understood. This means that one cannot change even the pseudotype without disrupting replication or control of the viral genome. As a result, we have decided to adopt technology that is currently showing clinical promise for gene therapy: the Conditionally Replicating Adenovirus vector that is not only oncolytic when it replicates within tumor cells but also can deliver a shRNA into neighboring cells that do not lyse. Conditional Replicating Adenoviruses (CRAds) can propagate within a neoplasm since each infected cell produces 1K – 10K's of selectively replicating virus. Also recent data suggest that these viruses may selectively target distant sites of tumor after systemic injection in preclinical models and therefore provide better targeting to tumor at distant sites. To accomplish this selective targeting a best approach appears to be to use an adenovirus of serotype 5 in which the knob of the fiber that distinguishes the type 5 virus is replaced with a type 3 knob to create a hybrid that is termed an Ad 5/3 viral vector. We are fortunate to have Dr. Korokhov (please see his Biosketch) join us who has worked with Dr. David Curiel who is a leader in this field and has created the basic tools for assembling CRAds that may be useful for our purpose. Our intent is to keep working with lentivirus but also to develop a CRAd that has a modified serotype with an Ad5/3 capsid fiber that decreases hepatic distribution but also allows for efficient targeting of systemic tumors. This is critical to enhancing safety as well as improving targeting of tumor after systemic injection.

A further improvement to safety for a conditionally replicating virus is to make the virus respond only to the transcription factors that drive the cancer. Since we focus on the activation and transcription of NANOGP8, it is logical to use the promoter for NANOGP8 to drive selective replication of the viral vector. There are two main strategies employed to restrict replication of adenoviruses to cancer cells; either expression of viral genes critical for viral replication are placed under the control of tumor-specific promoters or, viral genes required for replication in normal cells are modified to make them dependent on tumor gene expression. The first approach most often relies on a cancer-specific promoter to control transcription of the E1 region. Since NANOGP8 appears to be expressed only in malignant cells and not in normal cells (except for 1 report in smooth muscle cells, its promoter is likely to be able to control viral genes necessary for replication and will constrain viral replication so that it is restricted to malignant cells in our preclinical studies. In addition, we have shave shown that shRNA to *NANOG* or *NANOGP8* inhibits stem cell function as well as tumor growth both in vitro and in vivo. The critical steps to making a CRAd that replicates within the colorectal carcinoma xenograft are: 1) to identify a promoter that is selectively active within the cancer but not in normal tissue and strong enough to drive adenoviral

replication, 2) to insert this promoter into the adenoviral vector along with the shRNAs that we have developed, 3) to demonstrate that the CRAds amplify within 3-D suspension CRC cell cultures and 4) to use the CRAds to treat xenografts in vivo. We have the NANOGP8 promoter reporter construct of Jeter et al (18) that is active in both monolayer and spheroid cultures (Figure 8, Appendix I). Since this promoter construct is 3.8 Kb. we are currently testing whether shorter constructs that are closer to the 3' end may be active. Testing promoter activity is by simple transfection. Once an active construct is identified, then it will be inserted into the pShuttle vector AdEasy-1 as diagramed in Figure 9 and, along with a rescue vector containing the H1 driven shRNAs CRAd genomes will be assembled by homologous recombination within the E. coli designed for this.

Dr. Korokhov has the expertise (please see Biosketch) to create the CRAd5/3 by January 2014 using the promoter for NANOGP8 that we have in hand along with the shRNAs that we have shown are active in vitro. We have the assays developed to assess the ability of a CRAd5/3 to grow in human CRC in spheroids as well as xenografts so that it should not be difficult to complete the milestones for task 3. Thus, we are confident that we can develop a vector by the end of this grant that is ready for further preclinical testing.

We considered the possibility of using a replicating virus such as an oncolytic adenovirus. Dr. Korokhov had worked with Dr. David Curiel at the University of Alabama in Birmingham on the construction of different oncolytic adenoviruses. Adenovirus type 5 was the backbone of ONYX 15 that was a conditionally replicating adenovirus (CRAd) designed to proliferate in tumor cells that lost function of p53. Early trials demonstrated that the virus replicated in patients with head and neck squamous carcinoma but that host immunity limited the utility of systemically administered CRAd. Also type 5 adenovirus is hepatotoxic.

We designed adenoviruses with a chimeric fiber that combines a serotype 3 knob with a type 5 fiber to create a virus designated Ad5/3. Such chimeras have reduced hepatotropism (and hepatotoxicity). This Ad5/3 converts the receptor for the virus from the coxsackie adenovirus receptor (CAR gene) to desmoglein 2 (DSG2), a protein in hemidesmosomes expressed in epithelia and endothelial cells. The viruses that Dr. Korokhov made also contain H1-driven shRNAs (the control shNEG and the allele-specific shNG-1 and shNp8-1 along with the copGFP reporter driven by a CMV promoter) that were in the lentivirus. These wild type viruses will replicate in and lyse human cells but not mouse cells. The various viruses with the Wild Type (WT) promoter are Ad5/3-E1aWT-shNEG, Ad5/3-E1aWT -shNp8 and Ad5/3-E1aWT (this without shRNA or GFP reporter). Their design is shown in Figure 2 below with the upper panel describing the Ad5/3 WT (wild type genomes).

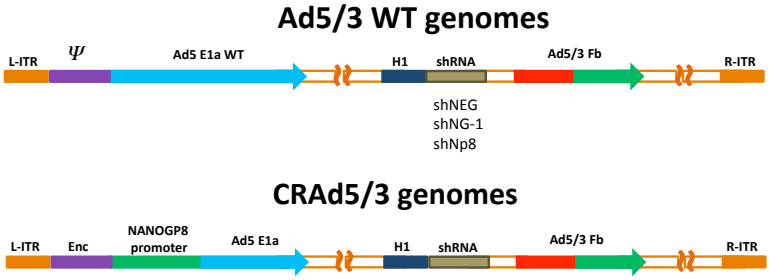

Figure 2. Design of Oncolytic Viruses (Upper Panel) and the CRAd (Lower Panel).

To make a conditionally replicating adenovirus with a 5/3 fiber (CRAd5/3) Dr. Korokhov replaced the Ψ and proximal part of the E1a gene with the proximal 1 Kb of the *NANOGP8* promoter. This minimal promoter contains consensus binding sites for a number of transcription binding sites that drive expression of *NANOGP8* and drive the rest of the E1a viral gene to initiate replication of the virus in cells that express *NANOGP8*. Therefore, a CRAd may only replicate in those cells that actively express *NANOGP8*. Ambady et al[1] demonstrated that *NANOGP8* is not expressed in normal cells in patients except some smooth muscle cells. The Ad5/3 WT and CRAd5/3 viruses will infect both mouse and human cells but replicate in and lyse human cells. The CRAd is Ad5/3-E1aNp8-shNp8. Interestingly, attempts to generate a CRAd5/3 that expresses shNG-1 did not mature into a lytic, plaque-forming virus.

The Ad5/3's with wild type promoters were first tested with Ad5/3-E1aWT and Ad5/3-E1aWT-shNp8 in Clone A and CX-1 at various dilutions of viral particles per CRC cell. As expected, increasing the titer of virus increases the infection rate as represented by the GFP fluorescence (Figure 3). Even at rates of only 1 or 3 viral particles per cell the Ad5/3 infects occasional cells that will eventually lead to infection of the majority of CRC cells. Also a transduction unit averages 13 viral particles per cell for all of the constructs that Dr. Korokhov has made.

[1] Ambady S1, Malcuit C, Kashpur O, et al. Expression of NANOG and NANOGP8 in a variety of undifferentiated and differentiated human cells. Int J Dev Biol. 2010;54(11-12):1743-54.

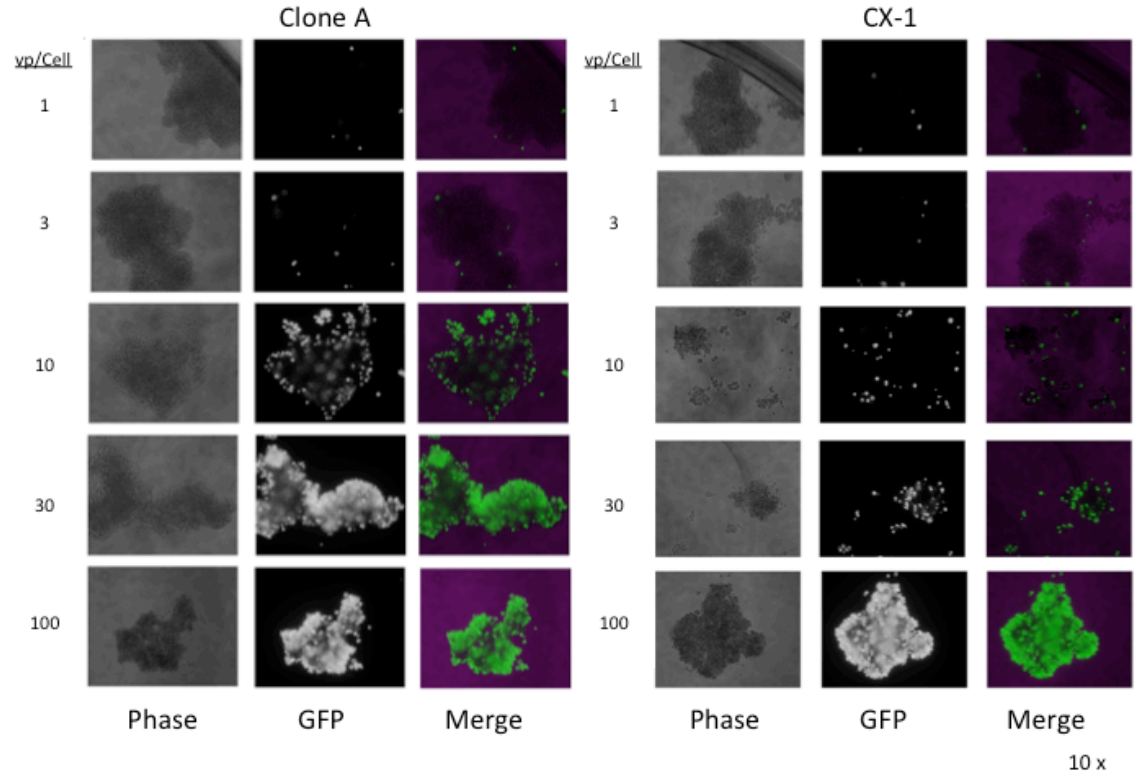

Figure 3. Infection of CRC in 3-D Suspension Culture. *500 Clone A or CX-1 cells were incubated in 96 well ultra low attachment (ULLA) in serum-free medium (SFM) plates for 24 hr before the indicated numbers of Ad5/3-E1aWT-shNp8 viral particles were added to the cultures. 6 days later cells were imaged with a 10x objective on a Nikon Diaphot inverted microscope.*

Representative results are shown below and demonstrate the utility of the replicating virus. In our LV experiments we achieved a maximal decrease in CRC cell survival of ~50% inhibition at 3 days. Since the LV is non-replicating, the untransduced cells will eventually grow even though we have demonstrated that the regrowth potential of CRC cells treated in 3-D cultures is decreased by about 30%. In contrast, exposure to Ad5/3-E1aWT or Ad5/3-E1aWT-shNp8 decreases cell survival over 10 days to <20% of that of the untreated control cells (Figure 4).

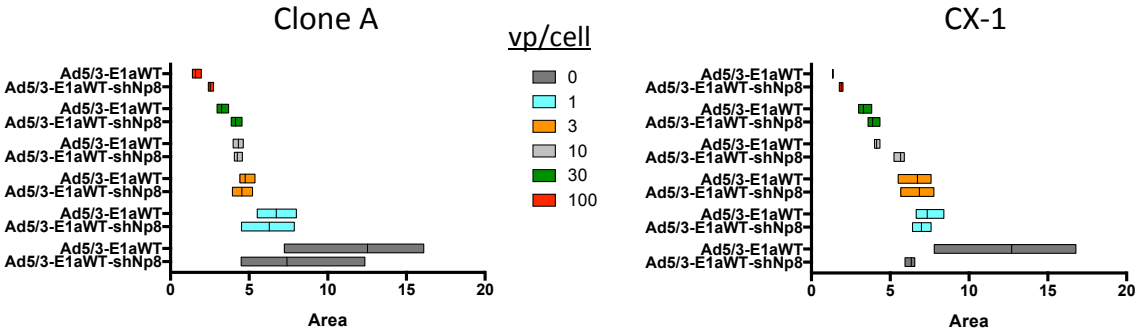

Figure 4. Adenoviruses inhibit growth of Clone A and CX-1 in Suspension Culture at 7 Days. *10^3 CRC cells in 96 well ultra low attachment plates in serum-free medium were exposed 16 hours after incubation with the titers of the indicated viruses at the viral particles per cell. After 7 days of infection the mass areas of culture were measured and means ± SD presented. Separate experiments indicate that area measurements correlate with Alamar Blue post labeling metabolism study (see below). The 30 and 100 vp/cell are at least P<0.01 versus the untreated controls.*

A major advantage of the replicating type of Ad5/3 is that as cells lyse they release up to 10,000 mature viruses that then infect neighboring cells. Wild type Ad5/3 will only replicate in human xenografts in murine preclinical models However, both the wild type Ad5/3's and the CRAd amplified in CRC growing in CX-1 in suspension, indicating the potential for oncolysis over time.

Modeling the Effect of Mouse Stroma on Ad5/3 Function

As we were preparing the CRAd for in vivo experiments, we tested whether murine fibroblasts affected the ability of the Ad5/3 to kill CRC cells. For this we used a 3T3 cells where Ad5/3 attaches but does not replicate. This is confirmed in co-culture experiments with CX-1 and LS 174T in which 500 CRC cells were incubated with 100, 250 or 500 3T3 cells or without 3T3 cells or no CRC with only 500 3T3 cells (Figure 5). As shown, 3T3 cells infected with 100 vp/cell do not express the GFP reporter that requires viral replication. In contrast, cells infected with Ad5/3-E1aWT-shNp8 do express the GFP reporter even at a 1:1 ratio of tumor cells to murine fibroblasts (Figure 5). These results suggest that while murine fibroblasts may act as a sponge for virus, the virus will infect susceptible cells and multiply. While infectivity of CX-1 was not affected by increasing concentration of 3T3, it

appears that the relative infection rate of LS 174T decreases with increasing 3T3 concentration. This may occur because LS 174T forms tight junctions that may 'hide' the DSG2 as it forms spheroids that exclude 3T3 fibroblasts. This exclusion has been confirmed by confocal imaging (Data Not Shown). It is not clear that this may occur in vivo in preclinical models or in patients.

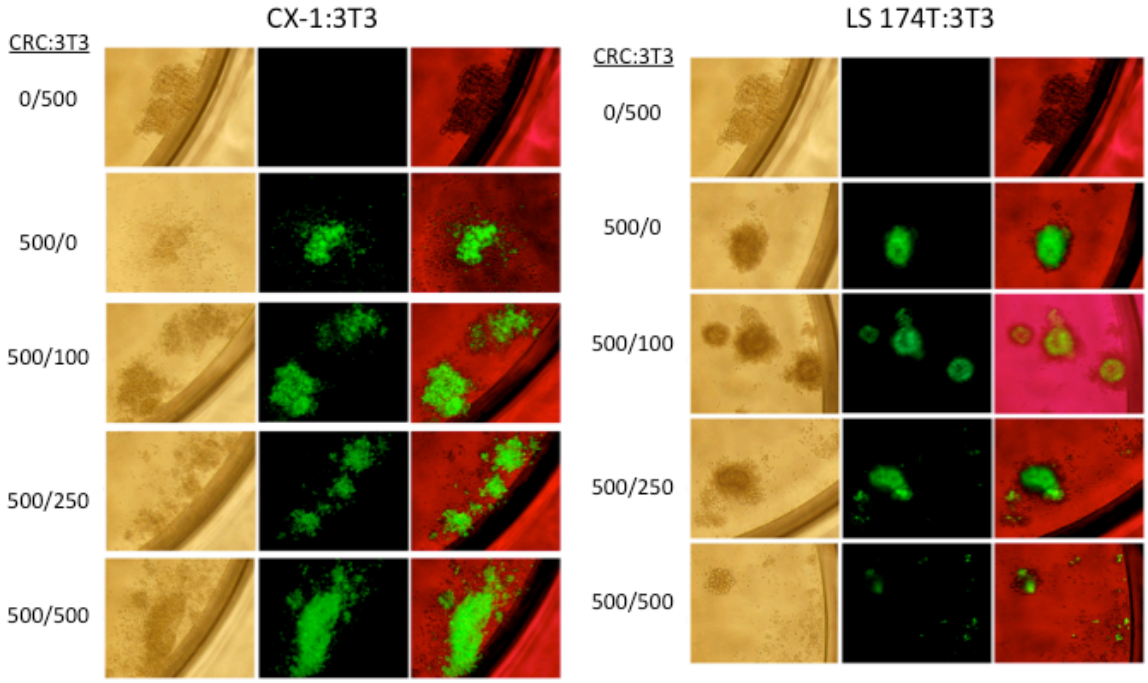

Figure 5. Effect of Murine 3T3 Fibroblasts on Infectivity of Ad5/3-E1aWT-shNp8. *The indicated numbers of CX-1, LS 174T and 3T3 cells were incubated for 16 hr in 96 well ULLA plates in SFM and infected with 100 vp/ CRC cell and imaged at days as described above in Figure 7. The 3T3 alone culture was also infected at the same titer as the CRC containing cultures. All cultures performed in triplicate.*

When the co-cultures were analyzed with the post assay viability dye Alomar Blue, there was an interesting effect of 3T3 on survival of CX-1 and LS 174T (Figure 6). The results indicate that in the absence of 3T3 cells both CX-1 and LS 174T are quite sensitive to Ad5/3-E1aWT-shNp8 but less sensitive to Ad5/3-E1a that lacks the shRNA (Figure 9). In addition, it is clear that the efficacy of the Ad5/3's decreases when the ratio of tumor cells to 3T3 cells drops to 2.5 or 1 tumor cell to 1 3T3 cell. These results suggest that Ad5/3's may be active in epithelial cancers where the stromal fibroblast to tumor cell ratios of 1:4 or lower. These experiemnts also suggest that the shRNA to *NANOGP8* may increase the efficacy of the Ad5/3 (Figure 6). The other consideration is that human stroma will support Ad5/3 replication so may augment tumor control. We are in the process of obtaining cancer – associated fibroblasts to see if these stromal cells may enhance the control of tumor cells in vitro and in preclinical models.

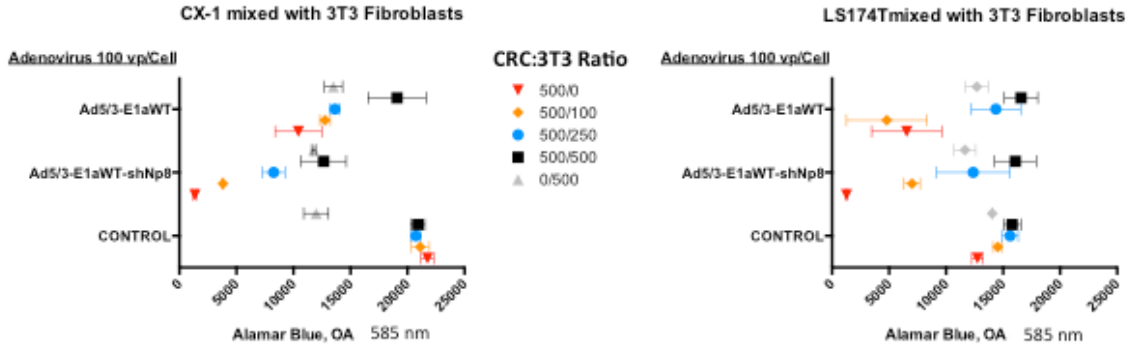

Figure 6. Effect of Murine Fibroblasts and shNp8 on CRC Survival. *As described in Figure 5, CX-1 and LS 174T cells were incubated in ULLA microtiter palates in SFM and infected with 100 viral particles (vp) per cell. Plates were incubated with Alomar Blue and then read in a microplate reader at 585 nm. Means ± SD are presented.*

Development of the CRAd5/3-E1aNp8-shNp8

Development of the *NANOGP8* driven CRAd took longer than expected. This was because the creation of the promoter construct by homologous recombination from the Ad5/3-E1aWT-shNp8 was slow. Similar CRAds with the *NANOGP8* promoter for the other shRNAs have not been successful despite multiple attempts. It is likely that since the adenoviral genome is relatively small,

the replacement of the wild type promoter with exogenous DNA may be a t the limit of the genome's ability to handle foreign DNA. Nonetheless, CRAd5/3-E1aNp8-shNp8 is active, replicates in 293T17 cells and CRC and is capable of killing human CRC as shown below. The first test of the ability of this virus to infect CX-1 and then release active viral particles that lyse fresh second cultures of either CX-1 or 293T17 cells is shown (Figure 7). These data suggest that the CRAd will amplify in human CRC and then are capable of secondary subsequent infection.

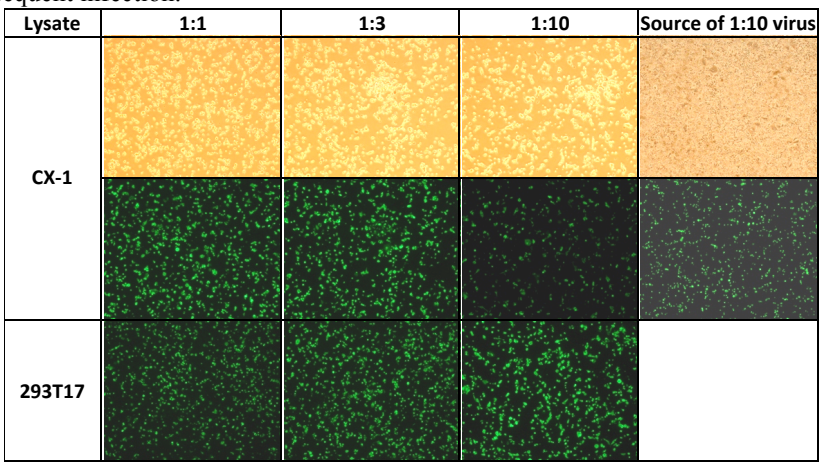

Figure 7. Lysate From CRAd-infected CX-1 infects Secondary CX-1 and 293 Cells. *CX-1 cells were infected with Ad5/3-E1aNp8-shNp8 (the CRAd) for 48 hr in monolayer culture, harvested, washed and a lysate prepared by repeated freeze thawing. This cell lysate was diluted 1:10 and then added to fresh monolayers of CX-1 or 293T17 cells at the further dilutions indicated. Phase and epi-fluorescence images were taken with a 4x objective on a Nikon Diaphot inverted microscope 48 hr after secondary infection. 293T17 cells contain E1a wild type and support the replication of adenovirus.*

We then further assessed the ability of the CRAd to infect CRC as well as to induce cell death by comparing the CRAd to AD5/3-E1aWT-shNp8 for transmission between cells and induction of Annexin V positivity over the course of 7 days in a CX-1 suspension culture. The *NANOGP8* promoter driven CRAD increased its infectivity 6-fold at 30 vp/cell and 2-fold at 100 vp/cell while Wild Type E1a-driven Ad5/3 increased its infection rate by 1.5-fold at 30 vp/cell and actually decreased its infection rate at 1000 vp/cell (Figure 8A and B). The CRAd induced Annexin V positivity 10 days after infection but the level is clearly lower than what is observed with either of the wild type Ad5/3s (Figure 8C).

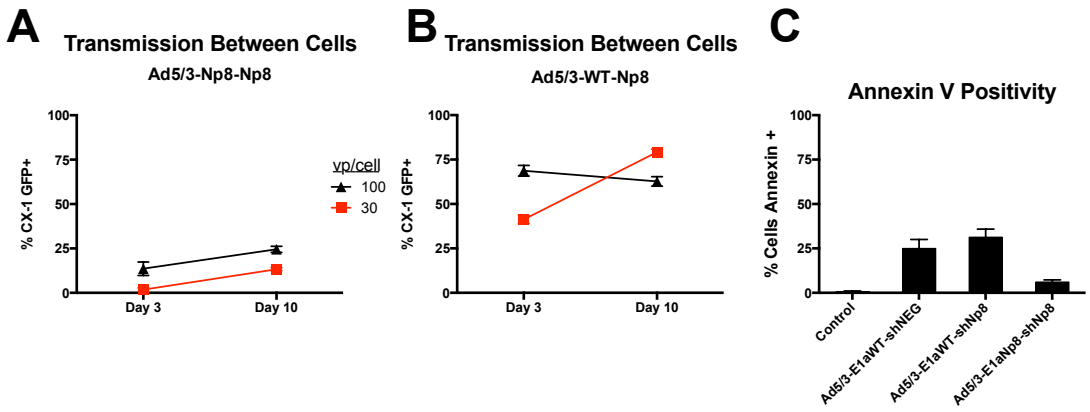

Figure 8. Transmission Between CX-1 Cells and Annexin V in CX-1 Suspension Culture. *CX-1 cells were incubated overnight in ULLA plates in SFM and then infected with dilutions of Ad5/3's for 10 days. Images were taken at 3 and 10 days after infection and the percentages of cells infected and expressing GFP were counted. Results are expressed as Mean ± SD of cells that are GFP+. Panel A is CRAd 5/3 while Panel B is the Ad5/3. Panel C is the percentage of cells that express Annexin V 6 days after infection of CX-1 cell in suspension culture with the indicated virus at 1000 vp/cell.*

When the CRAD was compared for inhibition of growth in the suspension culture model, it inhibited Alamar Blue metabolism significantly but not as much as the two wild type Ad5/3 viruses (Figure 9). These data indicate that lytic Ad5/3 viruses efficiently kill CX-1 cells. The CRAd5/3 was less efficient and active only at the 1000 viral particles per cell (~75 transduction units per cell). Thus, in the *in vitro* suspension culture system the CRAd5/3 was not as active as the wild type Ad5/3 and the shRNA was not more active than the control. Both results are explained by the different levels of transmission of adenovirus to secondary cells in cultures as well as reduced expression of Annexin V in the CRAd5/3 infected cells.

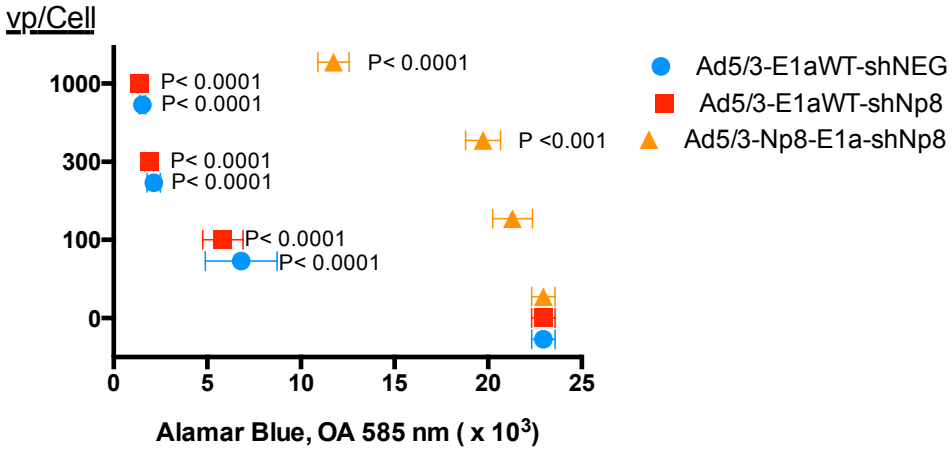

Figure 9. CRAd Has Activity at High Concentration. *CX-1 cells were infected at the vp/cell ratios indicated in Figure 7 above. The CRAd is Ad5/3-E1aNp8-shNp8 and indicated gold triangles. Triplicate cultures were analyzed for tumor area 6 days after culture iinfection and means ± SD presented. One way ANOVA was performed and highly significant and means compared by Holm-Sidak multiple comparisons correction test. P values compared to the untreated controls..*

CRAd and Ad5/3's Are Active in vivo

However, we tested the effect of the CRAd and the Ad5/3's in vivo in the CX-1 CRC. CX-1 cells were infected for 3 hours and then admixed with uninfected CX-1 cells before injection so that a total of 3 x 10^6 cells were injected so that only 5% or 50% of the cells were infected ex vivo. This tests whether cells infected with an Ad5/3 or CRAd can infect adjacent uninfected cells to inhibit tumor outgrowth. As expected, both the wild type Ad5/3 with or without shNp8 inhibited the growth of CX-1 cells (Figure 10). The weak inhibition of Ad5/3 wild type promoter with shNEG to inhibit CX-1 growth was a surprise and suggests that the control shRNA may have some effect that enhances tumor growth (Figure 10). Interestingly, the CRAd inhibited the growth of CX-1 when 50% of the cells were infected with a weaker but still significant effect when only 5% of the cells were infected (Figure 10). These results suggest that 1) the CRAd is active in preclinical models and 2) the shNEG control may interfere with inhibition of CRC in NOD/SCID mice, but do not necessarily show that shNp8 contributes to tumor inhibition since the most active adenovirus is the wild type Ad5/3 without shRNA. The activity of the CRAd *in vivo* may be related to the expression of the *NANOGs* that may be greater than even in suspension cultures. This is being actively investigated at this point.

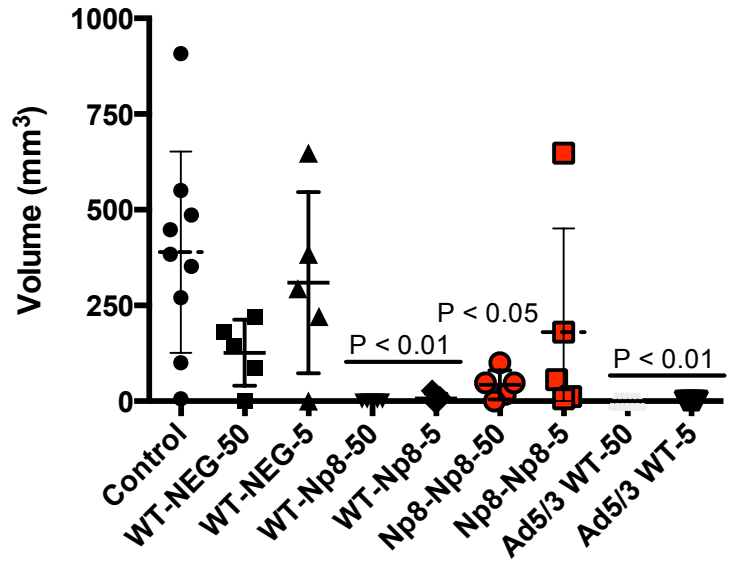

Figure 10. Effect of CRAd (Np8-shNp8) and Ad5/3's after ex vivo infection on Xenograft Growth of CX-1 in NOD/SCID Mice. *CX-1 cells were infected with the indicated virus for 3 hours and then admixed with uninfected CX-1 cells before injection so that a total of 3 x 10^6 cells were injected into groups of 5 mice each with only 5% or 50% of the cells infected ex vivo. Mice were followed and the results 18 days after transplantation are presented. The CRAd is designated Np8-Np8 for Ad5/3-E1aNp8-shNp8 and the other viruses have the wild type E1a promoter either without an shRNA (Ad5/3-WT), shNp8 (WT-Np8) or the control shNEG (WT-NEG).- Volumes were calculated by the formula width*width*length/width and expressed as mm^3. Mean ± SEM are presented. One-way ANOVA indicated that means were significantly different and then the means were compared by the Holm-Sidak multiple comparisons correction test. P values are compared to the untreated controls.*

With the no cost extension that we have requested we will be able to answer the questions posed by the Tech Transfer Review Group as well as to establish whether the CRAD and Ad5/3's are active in vivo.

Other Research Using LV shRNA's to *NANOG* and *NANOGP8*

We have submitted a manuscript that demonstrates that inhibition of the *NANOG/NANOGP8* gene expression inhibits MCL-1 expression as well as the expression of AKT and its activation. This effect potentiates the efficacy of BH3 peptides both *in vitro* and *in vivo* in a systemic treatment model in NOD/SCID mice as well as inhibiting the ability of CSC to support clonogenic regrowth. This is currently under review at *Clinical Cancer Research* (Mattoo AR, Jingyu Zhang J, Luis A. Espinoza LA, Jessup JM. Inhibition of NANOG/NANOGP8 results in MCL-1 down regulation in colorectal cancer cells to enhance the therapeutic efficacy of BH3 mimetics.). This has led to a follow-up study in which the CSC inhibitor selinomycin is used in place of shRNA to the *NANOGs*. The drug also potentiates the effect of the BH3 inhibitors in 3 of 4 human CRC cell lines. The 1 cell line that selinomycin does not affect is the one in which it does not inhibit MCL-1. Treatment with shNp8 did inhibit MCL-1 in all 4 lines and increased the activity of ABT-737 and ABT-199. We are now using Nanostring gene expression arrays to assess how shRNA alters gene expression.

Last year we reported that the LVshRNAs to the *NANOG*s potentiate the activity of Topotecan on CRC. This has not been published because the molecular mechanism is still unclear and we focused on the interaction between the *NANOGs* and BH3 death proteins.

We have found that inhibition of *NANOGP8* by LV shNp8-1 activates Caspase 9 and the intrinsic pathway of apoptosis during apoptotic stress caused during culture in suspension in serum-free medium in ULLA plates. This pathway is the subject of a manuscript under review (Mattoo AR, Zhang J, Espinoza LA, Korokhov N, Jessup JM. Inhibition of NANOGP8 or NANOG Activates the Intrinsic Pathway of Apoptosis. *Under revision*) and may also help increase the activity of drugs that may benefit from caspase-dependent cell death. Preliminary results with the Nanostring gene expression system suggests that inhibition of *NANOG* or *NANOGP8* leads to the alteration of 5 – 10 important transcription factors that then lead to secondary modifications in gene expression. Preliminary work suggests that in some CRC lines shNp8-1 and to a lesser extent shNG-1 activate autophagy and that this also leads to apoptosis when the level of autophagy is quite high.

In addition, we have begun to perform gene expression analyses with the Nanostring nCounter system using a panel of 770 cancer-associate genes. The purpose of this is to determine what changes in expression and pathways are actually altered by shRNA to *NANOGP8* and *NANOG*. Doing experiments in triplicate and using nonnegative factorization (NMF) algorithms we have found that LV shNp8-, the anti-*NANOGP8* shRNA, does indeed induce gene expression changes in monolayer that distinguish Clone A and CX-1 cells treated with LV shNp8-1 from cells treated with shNG-1 or the control shNEG (Figure 11).

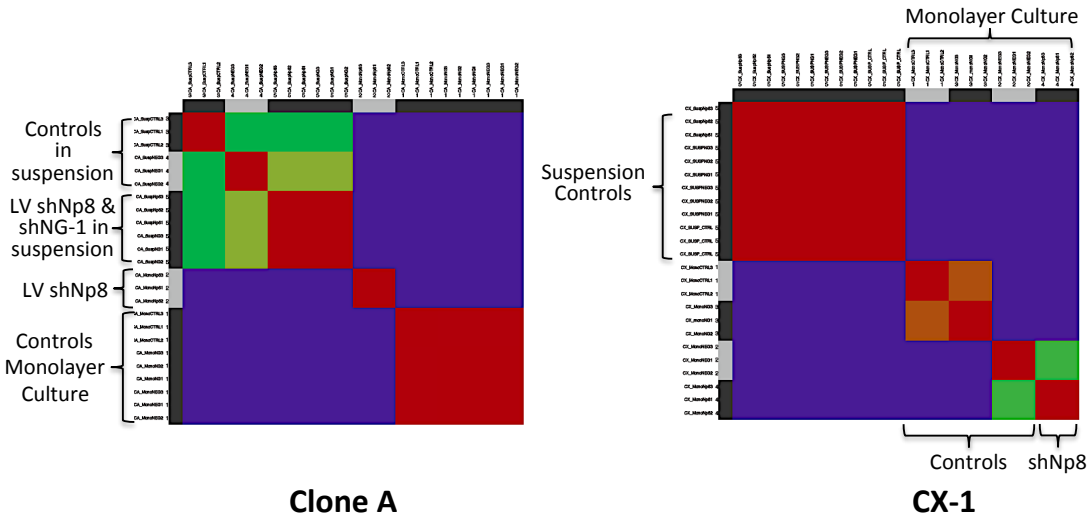

Figure 11. NMF Analysis of Gene Expression Profiles (GEP) Demonstrates the Effect of LV shNp8-1 on CRC Cells. *LV shRNAs were added to monolayer and suspension cultures at MOI of 5 for 48 hrs. Cultures were harvested, RNA isolated and GEP analysis performed with the Nanostring nCounter system using the 770 gene cancer panel. The GEPS were then analyzed by the NMF clustering program from the Broad Institute and the results of this unsupervised clustering with k=5 tuples is presented. LV shNp8-1 creates a distinct subset of GEP in monolayer culture in both CX-1 and Clone A cells.*

Since NMF does not indicate what genes are differentially expressed, we have then used comparative marker selection to identify those genes whose expression is altered with a P value of less than or equal to 0.001 and a false discovery rate (FDR) of less than or equal to 1% between cells treated with shNp8-1 or left untreated. All NMF and other algorithms and tests were performed on the Broad Institute public server. The results indicate that shNp8-1 down regulates XX genes and up regulates YY genes at this level of stringency while in Clone A AA genes and BB genes are up- or downregulated respectively (Figure 12, next page). Interestingly, the overlap is minimal. Also of interest is that with the unbiased or supervised clustering of the NMF program growth in suspension swamps the effects of the LV shRNAs, even though we have shown that LV shNp8-1 inhibits CRC growth in suspension culture by 50%. Further work is ongoing in this area and we hope to complete this if we receive a no cost extension.

Genes	Down	Up	Total
CX-1	74	55	129
Clone A	24	24	48

Genes in Common

	Clone A	
CX-1	Down	Up
Down	6	1
Up	1	5

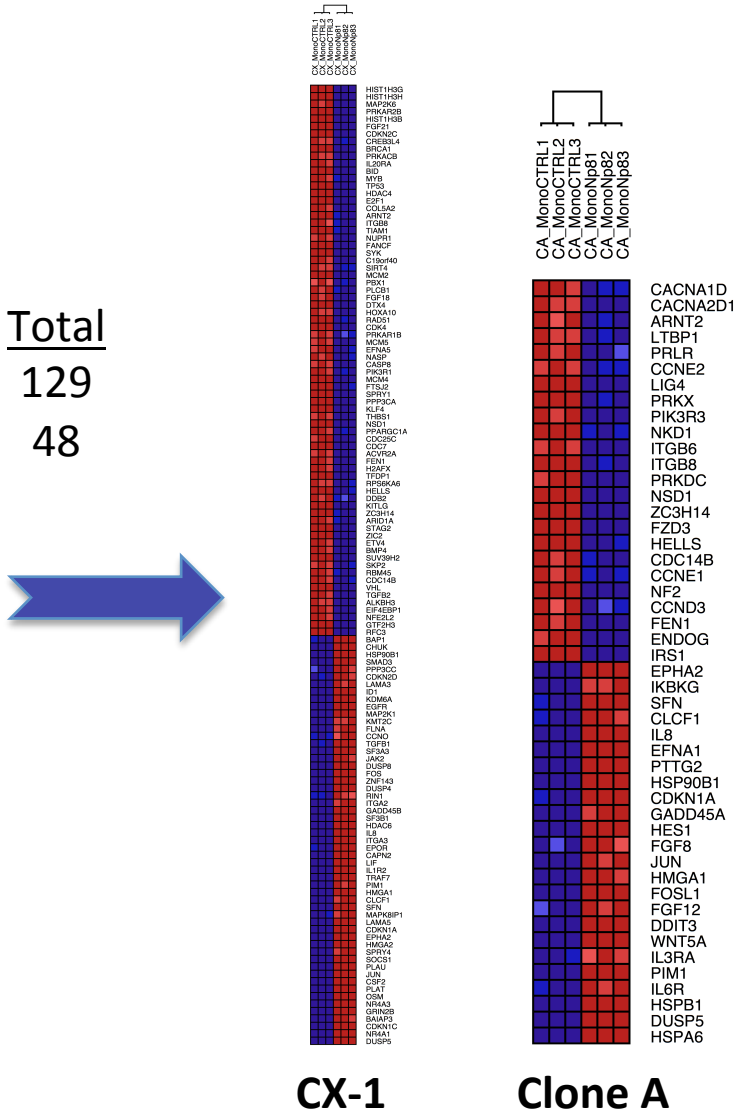

Figure 12. Expression Profiles of Genes Affected by LV shNp8-1 in Clone A and CX-1 human CRC Cells. *The GEPs from Figure 11 above for the monolayer cultures of CX-1 and Clone A untreated and LV shNp8-1 treated cells were analyzed in the Comparative Marker Selection program of the Broad Institute on the public server at the GenePattern.org website. The genes above were selected for a P value of less than or equal to 0.001 and a FDR of 1% as well as a decrement of 0.5 or greater for decreased expression or an increase of 2.0 or greater for LV shNp8-1 treated cells compared to intreated parental cells*

Products, Conclusions, Manuscripts, & Presentations

- Confirmation that NANOG is expressed in the majority of primary human colon carcinomas and that its expression is a significant prognostic factor, especially when associated with expression of the cell adhesion scaffold protein NEDD9.
- Elucidation of a molecular mechanism by which inhibition of NANOGP8 and/or NANOG induces apoptosis through inhibition of MCL-1 by Dr. Mattoo
- Proof of the principle that vector-delivered shRNA to NANOGP8 and/or NANOG inhibits MCL1 expression and enhances the efficacy of BH3 peptidomimetics to kill human colorectal cells.
- Confirmation that intralesional injection of LV-delivered shRNA to NANOGP8 or NANOG transduces tumor cells within xenografts growing in vivo in NOD/SCID mice.
- Demonstration that LV shNp8-1 (and LV shNG-1) induce gene expression changes that distinguish CRC cells treated in monolayer culture from CRC cells either not treated or treated with a control shRNA.
- creation of chimeric oncolytic adenoviruses that driven by wild type E1a viral genes contain the 5/3 fiber as well as either control shNEG or shNp8-1.
- creation of a conditionally replicating (CRAD) oncolytic adenovirus that has the same 5/3 fiber and the H1-driven shNp8-1 but is driven by a mini-promoter from the *NANOGP8* promoter.
- demonstration that CRAD and the oncolytic adenoviruses are active in vitro and in vivo in preclinical CRC models.

Manuscripts

1. Zhang J, Espinoza LA, Kinders RJ, Lawrence SM, Pfister TD, Zhou M, Veenstra T, Tang DG, Jeter C, Thorgeirsson SS, Jessup JM. Nanog modulates stemness in human colorectal cancer. *Oncogene. 2013 Sep 12;32(37):4397-405.* PMCID: PMC3556342
2. Mattoo AR, Zhang J, Espinoza LA, Jessup JM. Inhibition of NANOG/NANOGP8 down regulates MCL-1 in colorectal cancer cells and enhance the therapeutic efficacy of BH3 mimetics. *Clin Cancer Res. 2014 Sep 10.* pii: clincanres.1134.2014. (Available online – PMCID in process - Appendix)
3. Mattoo AR, Zhang J, Espinoza LA, Korokhov N, Jessup JM. Allelotypic Inhibition of Embryonic Transcription Factor Decreases Three-Dimensional Growth of Colorectal Carcinoma. *Under Revision.*- Appendix.

Presentations in 2013-2014

1. Mattoo AR, Korokhov N, Jessup JM. Inhibition of NANOGP8 or NANOG Activates the Intrinsic Pathway of Apoptosis. Presented May 22, 2014 at the Annual Meeting of the American Society of Gene and Cell Therapy, Molecular Therapy, 22:Suppl 1: abs 455, s175, 2014.

2. Mattoo AR, Thorgeirsson SS, JessupJM. Lessons Learned From TALEN Knockout Of *NANOG* In Colorectal Carcinoma (CRC) Cells. Presented May 23, 2014 at the Annual Meeting of the American Society of Gene and Cell Therapy, Molecular Therapy, 22:Suppl 1: abs 561, s217, 2014.

Inventions, Patents & Licenses

None.

Reportable Outcomes

None.

Other Achievements

None.

References

None.

Inhibition of *NANOG/NANOGP8* down regulates MCL-1 in colorectal cancer cells and enhances the therapeutic efficacy of BH3 mimetics.

Abid R. Mattoo[1], Jingyu Zhang[1], Luis A. Espinoza[1], J. Milburn Jessup[1,2,3]

[1]Laboratory of Experimental Carcinogenesis
Center for Cancer Research
National Cancer Institute

[2]Cancer Diagnosis Program
Division of Cancer Treatment and Diagnosis
National Cancer Institute

[3]Point of Contact: J. Milburn Jessup, MD
4W410
Bethesda, MD, 20892-7430

The authors are employees of the Federal Government and declare that they do not have financial conflicts of interest.

Keywords: *NANOGP8, NANOG*, colorectal carcinoma, apoptosis, BH3 mimetics, MCL-1

Running Title: *NANOGP8* Inhibition enhances BH3 mimetic efficacy

Translational Relevance:

Colorectal carcinoma (CRC) is the second leading cause of cancer death in US with recurrence occurring in 30-50% of stage II and stage III CRC patients after surgery and adjuvant therapy that is resistant to chemotherapy. Inhibition of the stem cell transcription factor *NANOG* or its retrogene *NANOGP8* decreases stemness and proliferation in CRC. Since high levels of BCL2 family proteins are expressed in CRC, we hypothesized that inhibition of *NANOG/NANOGP8* will decrease levels of prosurvival protein MCL-1 to enhance cytotoxicity of BH3 mimetics that target BCL2 proteins. Combining shRNA against *NANOG/NANOGP8* with BH3 mimetics decreased MCL-1, increased caspase-dependent apoptosis of CRC in vitro and inhibited CRC xenograft growth in vivo more than treatment with BH3 mimetics alone. Inhibition of *NANOG/NANOGP8* may reduce the addiction of CRC to MCL-1 and enhance the effect of BH3 mimetics.

Abbreviations

CRC (Colorectal Carcinoma), LV shNG1 (Lentivirus shRNA *NANOG*), LV shNp81 (Lentivirus shRNA *NANOGP8*), LVshNEG (Lentivirus shRNA *NEG*).

Translational Relevance: 136 words

Abstract: 247 words

Text: 4,015 words

Figures: 6 – all black & white

Supplementary Figures: 3

Supplementary Table: 1

Pages: 25

Abstract:

Purpose: High levels of BCL-2 family members in colorectal carcinoma (CRC) cause resistance to treatment. Inhibition of *NANOG* or its paralog *NANOGP8* reduces the proliferation, stemness and tumorigenicity of CRC cells. Our hypothesis was that inhibition of *NANOG/NANOGP8* enhances the cytotoxic effect of BH3 mimetics targeting BCL-2 family members in CRC cells through reducing expression of MCL-1, a prosurvival BCL-2 protein.

Experimental Design: Lentiviral vector (LV) shRNA to *NANOG* (shNG-1) or *NANOGP8* (shNp8-1) transduced CRC cells that were also exposed to the BH3 mimetics ABT-737 or ABT-199 in vivo in CRC xenografts and in vitro where proliferation, protein and gene expression, and apoptosis were measured.

Results: Clone A and CX-1 were sensitive to ABT-737 and ABT-199 at IC50's of 2-9 μM but LS174T was resistant with IC50's of 18-30 μM. Resistance was associated with high MCL-1 expression in LS174T. LVshNG-1 or LVshNp8-1 decreased MCL-1 expression, increased apoptosis and decreased replating efficiency in CRC cells treated with either ABT-737 or ABT-199 compared to the effects of either BH3 mimetic alone. Inhibition or overexpression of MCL-1 alone replicated the effects of LVshNG-1 or LVshNp8-1 in increasing or decreasing the apoptosis caused with the BH3 mimetic. The combination therapy inhibited the growth of LS174T xenografts in vivo compared to untreated controls or treatment with only LV shRNA or ABT-737.

Conclusions: Inhibition of *NANOGP8* or *NANOG* enhances the cytotoxicity of BH3 mimetics that target BCL-2 family members. Gene therapy targeting the NANOGs may increase the efficacy of BH3 mimetics in CRC.

Introduction:

Colorectal carcinoma (CRC) is the second leading cause of cancer death in the US without recent improvements in stage specific death rates. Chemotherapy is used for the adjuvant therapy of stage II and stage III CRC because it causes programmed cell death or apoptosis (1) . However chemotherapy may not kill CRC that express high levels of prosurvival BCL2 proteins (2-4). This supports development of new treatments to overcome the overexpression of these BCL-2 proteins (5, 6).

The BCL-2 family of proteins decides whether a cell continues to live or undergoes death through the intrinsic or mitochondrial apoptotic pathway. Multidomain BCL-2 ,BCL-XL.MCL-1,BCL-W and BFL-1 are the prosurvival members of the BCL2 family, whereas BAX,BAK and BOX are the pro-apoptotic members (7). Single domain BH3 only members of the family include PUMA,NOXA,BIM,BID,BAD,BIK that modulate the actions of the multidomain members (7). Various models explain how the BH3 only proteins affect the function of BCL-2 proteins regulating apoptosis (8, 9). This has led to the development of such BH3 mimetics as ABT-737 and ABT-199 that induce apoptosis in cancer cells. ABT-737 has high affinity to BCL-2, BCL-XL and BCL-W (10) whereas ABT-199 , a second generation BH3 mimetic, is a highly potent and specific inhibitor of BCL-2 (11). ABT-737 has shown good response in killing CRC cell lines as a single agent or in combination with chemotherapy(3, 12) while ABT-199 has shown strong activity against CLL, multiple myelomas and estrogen receptor positive breast cancers, either alone or in combination with other drugs. (13-15). However, neither molecule inhibits the other important prosurvival protein MCL-1. Thus, when MCL-1 is highly expressed in cancer cells, ABT-737 has shown activity only when used in combination with molecules which neutralize MCL-1 (3, 9, 16-19). At this point there seems to be little data on efficiency of ABT-199 in presence of MCL-1.

NANOG is a key embryonic transcription factor that maintains pluripotency (20, 21) and is located on chromosome 12. *NANOGP8* is a retrogene located on chromosome 15 that is expressed in a wide variety of cancers (22-25). Our group showed that inhibition of *NANOG* and its retrogene *NANOGP8* ablates stemness in human CRC as measured by reduced

spherogenicity, side population size, proliferation *in vitro*, and tumorigenicity and metastatic potential in NOD/SCID mice (26). *NANOGP8* may replace NANOG in supporting characteristics of stemness such as proliferation (22) and spherogenicity (26). Moreover, it was recently reported that inhibiting *NANOG* expression decreases MCL-1 protein levels indirectly through a decrease in the phosphorylation of AKT.(27)

We postulated that inhibition of *NANOG* or *NANOGP8* may inhibit MCL-1 expression in CRC and enhance the cytotoxicity of ABT-737 or ABT-199. Our approach was to test this *in vivo* in mice, in vitro in the WST-1 survival assay as well as to measure the effect of the agents upon caspase 3 and 7 activity as a direct measure of the induction of apoptosis. NANOG and NANOGP8 are essentially identical proteins of 305 amino acids whose coding regions differ by only 5 nucleotides that create nonsynonymous changes in 2 amino acids. Our allele specific shRNAs target codon 759 of *NANOG* (shNG-1) or *NANOGP8* (shNp8-1) (26) decreased MCL-1 expression and enhanced the cytotoxicity of the BH3 mimetics in the 3 CRC cell lines Clone A, CX-1 and LS 174T.

Material and Methods:

ABT-737 and ABT-199 were purchased from Selleck Chemicals LLC (Houston, Texas, USA). ABT-737 and ABT-199 and stocks in DMSO at 10mM/L were stored at -20°C. Lipofectamine 2000 for transfections was purchased from Invitrogen (Frederick, MD, USA). Polybrene and protamine sulfate for Lentivirus transduction and propylene glycol and Tween-80 were purchased from Sigma-Aldrich Chemical Co. (St. Louis, MO, USA). Precast NU-PAGE 4–12 % Bis Tris gels, NU-PAGE MES SDS Running Buffer and NU-PAGE transfer buffer were purchased from Invitrogen (Frederick, MD, USA). 96 –well white plates (ViewPlate-96 TC) for Caspase Glo assay were purchased from Perkin Elmer life sciences (Waltham, MA, USA). Caspase 3 inhibitor (Z-DEVD-FMK) was obtained from R & D systems (Minneapolis,MN,USA). MCL-1 overexpression plasmid pTOPO-MCL1 (Plasmid No 21605) was purchased from Addgene (Cambridge,MA,USA).

Cell culture, cell transfection, lentivirus packaging and cell transduction

Clone A is a subclone of the DLD-1 cell line. (26, 28) CX-1 is a highly metastatic variant of HT29 (28) and LS174T is a CRC cell line obtained from ATCC (Manassas, VA, USA) and used in our previous study (26). The cell lines were authenticated by the University of Arizona Genetics Core, Tuscon, Arizona (Supplementary Table 2). All these cell lines were cultured in RPMI (Invitrogen, Frederick,MD,USA) media supplemented with 10% fetal bovine serum (Invitrogen) and 2mM L-glutamine (Invitrogen) at 37°C, 5% CO_2 incubator. The Lentivirus particles containing the allele specific shRNA's for *NANOG* (shNG-1), *NANOG*P8 (shNp8-1) and negative control (shNEG) were produced by co-transfection of 293T cells with packaging and envelope plasmids using Lipofectamine 2000 (Invitrogen) as described (26). The transduction of the lentiviral particles at an MOI of 5-8 for all the experiments was done using polybrene or protamine sulfate as the transducing agent.

Tumors: Animal experiments were performed under the protocol LEC-052 approved by the NCI Animal Care and Use Committee. Three million viable untreated LS174T cells or LS174T cells transduced with shNEG, shNG-1 or shNp8-1 were injected subcutaneously into 8 groups of 5 5- to 6-week-old NOD/SCID male mice (Figure 1). ABT-737 was dissolved in 30% propylene glycol,

5% Tween-80, 3.3% D5W (pH 1.0), and 1% DMSO, sonicated,and pH adjusted to pH 4-5. When tumors reached ~100 mm^3, ABT-737 (100 mg/kg) was injected intraperitoneally daily for 5 days. Tumor volumes were calculated by the formula perpendicular length times $width^2$. Mice were sacrificed when the control tumor volume reached 2000mm^3 8 days later. Statistical analysis of the treated tumors relative to control was done using one-way ANOVA with Holm-Sidak multiple comparisons correction test in GraphPad Prism 6.

Assays: WST-1 (Roche Indianapolis, Indiana, USA) and Caspase-Glo (Madison, WI, USA) were used according to the directions supplied by the manufacturers. For the clonogenic or regrowth assay the 3 cell lines were seeded with 10,000 cells in a 48 well plate (Costar/Corning, Tewksbury MA, USA) in RPMI-1640 media with supplements. After 16 hr cells were treated with LV shNEG, LVshNG-1 and LVshNp8-1 or ABT-737 alone for 8 days or with one of the three shRNA's for 5 days followed by ABT-737 (2uM) for three more days. The supernatant was removed from the wells after 8 days and remaining adherent cells were trypsinized and an equal number of cells as described in the text were plated in 60 mm dishes with complete RPMI media, in duplicates for each treatment. The cells were incubated for 14 days and fixed and stained with 0.05% Crystal violet in 10% neutral-buffered formalin (37% vol), methanol (1%) and 0.15 M PBS (62% vol). The plates were washed with water and the colonies counted. For assessment of caspase function Caspase 3 inhibitor (Z-DEVD-FMK) was added 4hr after adding LV and ABT-737 at 10μM and then the cultures were analyzed by WST-1 assay as explained above.

Western Blot analysis: CRC cells were washed with PBS and then solubilized with RIPA buffer containing both protease and phosphatase inhibitors. Precast NU-PAGE 4–12% gels were used to separate cell lysates. Lysates transferred to Nitrocellulose membranes were probed with rabbit anti-MCL-1 (Cell Signaling Technology, Cat# 4572, Santa Cruz, Cat#sc819),BCL-2 (Cat#2876) ,BCL-XL (Cat#2762), NANOG(Cat#4903),AKT (Cat#9272),AKT-Ser473 (Cat#4060),, BCL-W(Cat#2724), and BIM(Cat#2819), and β-actin (Cat#4967) to monitor changes in the level of these proteins. The primary antibody was detected with goat anti-rabbit-HRP (Jackson Immunoresearch, West Grove, PA, USA).

Statistical Analysis: ANOVA was performed for statistical analysis of multiple comparisons using GraphPad Prism 6 (San Diego, CA, USA). Data in graphs are presented as mean ± S.D. except where indicated in the text. For the analyses, $P<0.05$ was considered to be statistically significant. All experiments were repeated at least twice independently.

Results:

Combination treatment of ABT-737 and LVshNG-1/ LVshNp8-1 in mice bearing LS174T xenografts:

In order to test the combination of ABT-737 with LVshNG1 and LVshNp81 *in vivo*, we injected NOD/SCID male mice with 3 x 10^6 LS174T cells transduced with LV shNG-1 or shNp8-1 or the control shNEG or left untreated. The ABT-737 treatment was started at Day 8 when the tumors were ~ 100mm^3. The mice were sacrificed at Day 17 when the tumors of the control groups of mice reached around 2000 mm^3. When tumors were analyzed at day 8 before the start of ABT-737 treatment, the levels of total NANOG transcripts in tumors initiated with LV shNG-1 or LV shNp8-1 were two-thirds or one-half, respectively of the transcript levels in the control tumors (Figure 1A). The volume of tumors of mice treated with the single agents of LV shNEG, LV shNG1, LV shNp8-1, or ABT-737 or the control combination of LV shNEG + ABT-737 was not significantly reduced compared to the size of the untreated controls (Figure 1B, C). However, the mean volume of tumors in mice treated with combined LV shNG1+ ABT-737 ($P<0.01$) or LV shNp81 + ABT-737 ($P<0.01$) was one-third that of the mean of the untreated controls (Figure 1C). These results support the postulate that inhibition of NANOG/NANOGP8 enhances the efficacy of ABT-737 in CRC xenografts. Further studies were performed in vitro to elucidate mechanism.

Colorectal Cancer (CRC) cell lines are variably sensitive to ABT-737:

We began these studies by determining the IC_{50} of ABT-737 on three cell lines (Clone A, CX-1 and LS174T). IC_{50} values were 7.5 µM for Clone A cells, 1.8 µM for CX-1 and high 18.3 µM for LS174T cells in a 48 hr viability treatment (Figures 2A-C). The protein levels of the prosurvival proteins BCL-2 (BCL2), BCL-xL (BCL2L1), MCL-1 (MCL1), BCL-W BCL2L2), and BIM (BCL2L11) were also analyzed (Figure 2D). LS174T cells express nearly three times the amount of MCL-1 as Clone A and CX-1 but the other prosurvival Bcl-2 family proteins are expressed similarly by the three cell lines (Figure 2D).

Enhanced killing via combinations of ABT-737 and LVshNG-1 and LVshNp8-1 in CRC cell lines:

Prior studies have demonstrated that inhibition of *NANOG* decreases cell proliferation, causes cell cycle arrest, induces apoptosis and inhibits stemness in a variety of cancer cell lines (26, 29). Conditional knockout of *NANOG* in mice induces apoptotic cell death in murine migrating primordial germ cells (30). We tested the combination of ABT-737 with LV shRNAs in these CRC cell lines at a concentration of 1 μM ABT-737. This concentration of ABT-737 by itself produced little or no cytotoxicity in Clone A, CX-1 and LS174T (Figure 3). The combination experiment was done to test also the timing of ABT-737 and shRNA on the response of CRC cells to the combination where CRC cells were exposed ABT-737 (1uM) for at least 3 days with exposure to LV shRNA for at least 5 days (Figure 3). In "ABT first" experiments, cells were treated first with ABT-737 (1 μM) for 3 days followed by treatment with LV shRNA's (LV shNEG, LV shNG-1 and LV shNp8-1) for 5 days. In "ABT Second" studies the three cell lines were treated with LV shRNA's for 5 days first followed by treatment with ABT-737 (1 μM) for 3 days. "ABT Continuous" studies represent the cell lines treated with ABT-737 and LV shRNA's simultaneously for 8 days. All combination treatments lasted 8 days. Cell survival was determined by metabolism of WST-1 and results presented as the Mean ± SD of the % of Control values of the untreated CRC cells after 8 days: fewer cells are associated with a lower amount of WST-1 metabolized (Figure 3). In Clone A the combination treatment (LV shNp8-1 + ABT-737) decreased cell survival by as much as by 40% relative to the lentiviral treatment control (LV shNEG + ABT-737) in all the combination therapy groups (Figure 3A) and LS174T cells had a similar decrease in survival relative to the lentiviral control shNEG but only when the cells were transduced with lentiviral shRNA first or concurrently with ABT-737 addition (Figure 3C). Interestingly, the CX-1 cells were only inhibited when the lentiviral shRNA was transduced first (Figure 3B). Since CX-1 is sensitive to ABT-737, the BH3 mimetic effect may mask the potential effect from inhibiting NANOG and/or NANOGP8. As a result, a dose response experiment with ABT-737 was performed with CX-1 cells treated with LV shNp8-1. The combination enhances the growth inhibition of CX-1 cells by reducing the IC50 of 2.8 μM for ABT-737 alone by more than 50% to 1.31 μM for the combination (Figure S1, $P<0.0001$). Also in each cell line shNp8-1 transduction was more active than shNG-1 in inhibiting growth (Figure 3A-C).

Killing of cells is associated with loss of MCL-1 and increase in Caspase 3/7 activity:

Inhibition of *NANOG* in cancer cell lines has been associated with loss of AKT phosphorylation and a decrease in MCL-1 levels (27). To elucidate whether enhanced killing associated with combination of LV shRNA against *NANOG* or *NANOGP8* and ABT-737 is associated with loss of AKT phosphorylation and decrease in MCL-1 levels due to inhibition of *NANOG*, we treated the three CRC cell lines with the LV-delivered shRNA. The inhibition of either *NANOG* or *NANOGP8* in Clone A cells resulted in a decrease in the levels of NANOG, phosphorylation of AKT at Ser-473, and in MCL-1 (Figure S2). Inhibition of *NANOG* and *NANOGP8* gene expression by shRNA did not decrease relative MCL-1 transcript levels (Figure S2 Panels A and B) but did decrease MCL-1 protein expression by at least 50% in all three CRC cell lines, whereas treatment with the control LVshNEG did not (Figure 4A). Caspase 3/7 activity was induced in Clone A, CX-1 and LS174T cell lines when CRC cells were cultured with 1 μM ABT-737 after first being pre-treated with LV shRNAs (Figure 4B). Transduction with LV shNEG, LV shNG-1 or LV shNp8-1 alone did not increase Caspase 3/7 activity (Figure 4B) whereas ABT-737 alone increased Caspase 3/7 activity significantly in CX-1 cells and to a lesser extent in Clone A treated for 7 days (Figure 4B). The combination of LV shNEG and ABT-737 increased Caspase 3/7 activity moderately 2-4 fold in the 3 cell lines (Figure 4B). However, in all 3 cell lines the combination treatment with LV shNG-1 or LV shNp8-1 increased Caspase 3/7 activity by 5.5 – 7.5 fold compared to untreated cells and more than that caused by LV shNEG and ABT-737 (Figure 4B). Inhibition of CRC growth induced by the combination therapy of shRNA and ABT-737 are associated with apoptosis as reflected by the activity of the executioner caspases. The inhibition of cell survival by combination therapy is caused by caspase-dependent cell death since addition of a caspase 3 inhibitor peptide blocked the cytoxic effect of LV shNp8-1 and ABT-737 (Figure 4C).

ABT-199 and its activity in CRC cell lines:

The IC_{50}'s for Clone A, CX-1 and LS174T treated with ABT-199 are 9.8 μM, 6.7 μM and 29.5 μM, respectively (Figure 5A). Clone A showed similar sensitivity to ABT-737 and ABT-199 (Supplementary Table 1). In contrast, CX-1 and LS174T were more sensitive to ABT-737 than ABT-199 (Supplementary Table 1). These patterns of differing sensitivity have also been observed in other cancer cell lines (14). To test the activity of ABT-199 in combination with LV

shNG-1 or shNp8-1 in these three CRC cell lines, the combination treatment was done in a similar manner as explained for ABT-737 above (Figure 5B). The concentration of ABT-199 used for this experiment was 2 μM. In Clone A and LS174T cells the combination treatment (LV shNp8-1 + ABT-199) resulted in the inhibition of cell growth by as much as 60% relative to LV control (LV shNEG + ABT-199) (Figure 5B). CX-1 survival was inhibited by 30% when treated with the combination (LV shNp8-1 + ABT-199) relative to control (LV shNEG + ABT-199). Inhibition of BCL-2 alone by a low concentration of ABT-199 enhances the inhibition of Clone A and LS 174T cells treated with LV shNG-1 or LV shNP8-1, especially if the ABT-199 is given after or continuously with the LV shRNA (Figure 5B).

Inhibition of *MCL-1* by siRNA increases Caspase 3/7 activity in CRC cell lines when used in combination with ABT-737/ABT-199:

We tested whether the effect of inhibiting *NANOG/NANOGP8* on augmenting the cytotoxicity of the BH3 mimetics depended on the reduction of MCL-1 protein expression by directly modulating the expression of MCL-1 and assessing sensitivity to the BH3 mimetics. CRC cells were transfected with siRNA *MCL-1* (100nM) alone or in combination with ABT-737/ABT-199 treatment. Transfection of the three CRC cell lines decreased MCL-1 by 3 – 6-fold (Figure 6A). Transfection of LS174T cells with only siRNA to *MCL-1* increased 2-fold the Caspase 3/7 activity whereas such transfection did not increase Caspase 3/7 activity in Clone A or CX-1 (Figure 6B). Treatment with ABT-737 induced Caspase 3/7 activity similar to what occurred earlier with inhibition of *NANOG/NANOGP8* (Figure 6B). ABT-199 alone induced Caspase 3/7 activity that was similar to ABT-737 in Clone A and LS174T cells (Figure 5B). In CX-1 cells ABT-737 induced more Caspase 3/7 activity than ABT-199 alone (Figure 6B). The combination of siRNA to MCL-1 with either BH3 peptide further increased Caspase 3/7 activity in each cell line (Figure 6B). In contrast, overexpression of *MCL-1* in LS174T cells rescued the growth of LS174T treated with the combination of LVshNp8-1 + ABT-737 (Figure 6C) while increasing the level of MCL-1 protein in all cells transfected with the MCL-1 (Figure 6D). Thus, direct modulation of MCL-1 expression mimics the effects of inhibition of *NANOG/NANOGP8* on BH3 mimetics on caspase activity and survival.

Clonogenic Regrowth assay:

The ability of lentiviral shRNA combined with ABT-737 to induce a long lasting inhibition of growth in the three CRC cell lines was determined by a colony forming assay (31) (Figure S3). CRC cells were treated with ABT-737, LV shRNA or the combination for 8 days and surviving adherent cells were collected and replated in fresh complete medium. In each experiment 500 viable cells were plated for each condition and then after 14 days stained and colonies counted. The combination of LV shNp8-1 and ABT-737 significantly decreased regrowth colony efficiency compared to the combination of ABT-737 and LVshNEG1 by 50 and 80% (Figure S3). The combination of ABT-737 and LV shNG-1 had a lesser effect. These data suggest that even those cells that survive to the end of original incubation period have a residual persistent growth inhibition from the combination therapy.

Discussion:

The inhibition of MCL-1 achieved through inhibition of *NANOGP8* or *NANOG* increases the growth inhibitory effects of the BH3 mimetics ABT-737 and ABT-199. ABT-737 has potent activity against leukemia and lymphoma cancer cell lines as a single agent and is also effective against multiple myeloma, glioma and small cell lung cancers (32). In CRC cell lines ABT-737 has shown poor efficacy as a single agent but the growth inhibition increases when ABT-737 is used in combination with other therapies (3, 5, 6, 12). In this study, the CRC cell lines exhibited low to moderate sensitivity when treated with ABT-737 or ABT-199 as single agents with CX-1 being the most sensitive cell line (Supplementary Table 1). LS174T cell line exhibited the greatest resistance (IC50 > 12uM) (Supplementary Table 1) towards both ABT-737 and ABT-199 associated with the higher expression of MCL-1. Our study demonstrates that the treatment of 3 CRC cell lines with the combination of LVshNG-1 orLVshNp8-1 and BH3 mimetics enhances the growth inhibitory effect in these cell lines. Earlier studies have also demonstrated that when small cell lung cancer (SCLC) cell lines are treated with a combination of ABT-737 and agents which decrease MCL-1 levels, ABT-737 resistant SCLC cell lines demonstrate enhanced killing compared to ABT-737 sensitive SCLC cell lines which show only moderate increase in cell killing when treated with the combination. (16)

Furthermore we also show that the inhibition of *NANOG*/*NANOGP8* alone decreases the levels of MCL-1 protein. Our finding extends the study of *Noh et.al.(27)* who demonstrated that *NANOG* promotes a stem-like and immune resistant phenotype in multiple types of cancer cell lines, including the HCT-116 CRC cell line. They elucidated that *NANOG* acts through TCL1A mediated AKT regulation of MCL-1 with knock down of *NANOG* decreasing the levels of pAKT and MCL-1. Although Boyer et al. (33) demonstrated that NANOG binds to the MCL-1 promoter, we have confirmed that inhibition of *NANOG* or *NANOGP8* does not change the levels of *MCL-1* transcripts (Figure S2A-B). However, inhibition of the *NANOGs* decreases pAKT (Figure S2C) and MCL-1 expression (Figure 4A) These results suggest that regulation of MCL-1 is a post-translational event. Moreover, when we treated the 3 CRC cell lines with the

combination of LV shNG-1 or LV shNp8-1 and ABT-737, it increased the Caspase 3/7 activity. Caspase 3 inhibition blocked the enhanced growth inhibitory effect of the combination (Figure 4C). We also demonstrate that the combination of siRNA *MCL-1* and ABT-737/ABT-199 increased the Caspase 3/7 activity in these CRC cell lines whereas overexpression of MCL-1 neutralized the growth inhibitory effect of the shRNA-ABT combination (Figure 6C). These findings further strengthen the finding that enhanced caspase 3/7 or growth inhibitory effect by combination of LVshNG-1/shNp8-1 and ABT-737/ABT-199 is the consequence of decrease in the levels of MCL-1. Thus, the combination of inhibition of *NANOG/NANOGP8* and the BH3 mimetic combination increased caspase-dependent apoptosis.

ABT-199 combined with LVshNG-1 and/or LVshNp8-1 treatment was ~20% more active than the combination with ABT-737 in Clone A and LS174T. Recent studies (11, 14, 15) also support this finding that ABT-199 is more potent than ABT-737 when used alone or in combination with other drugs. Furthermore, the combination of LV shRNA to *NANOG* or *NANOGP8* with ABT-199 reveals that the two agents administered together at the start of the experiment is more potent than when the treatments are administered sequentially (Figure 5). These findings suggest that the combination of inhibition of the *NANOGs* could be administered on the same day in the clinic rather than on separate days. This would simplify preclinical testing of this combination. The proof of the principle was validated in vivo with the demonstration that transduction of a CRC xenograft with either LVshNG-1 or shNp8-1 enhanced systemic therapy with a BH3 mimetic (Figure 1).

The clonogenic regrowth experiment performed in this study demonstrates that treating the CRC cell lines with ABT-737 alone (in Clone A and LS174T cells) or the combination of LVshNG-1 or LVshNp8-1 and ABT-737 (in all 3 cell lines) decreased the ability of the treated cells to regrow when replated in complete culture media. This experiment indicates that the CRC cells treated with these agents have reduced capacity to form colonies (clonogenicity) in normal media. Clonogenicity is associated with the stem cell nature of CRC (34) and the decrease in clonogenicity has been used as an indicator of a decrease in stem cell nature or self-renewal potential of different cancers (35-37). Inhibition of *NANOG* or *NANOGP8* decreases the

proliferation and self-renewal capacity of CRC and other cancers (26, 29, 38). Inhibition of anti-apoptotic BCL-2 family members by other BH3 inhibitors, ABT-263 and sabutoclax, selectively killed stem cells in leukemias (39, 40). Taken together these findings suggest that the combination of shRNA against *NANOG* or *NANOG* P8 and BH3 mimetics may target cancer stem cells and decrease the self-renewal capacity of these CRC cell lines.

In summary, inhibition of *NANOG* and *NANOGP8* by gene therapy combined with a BH3 mimetic may provide a rationale for new therapy regimen for colorectal cancers and target the stem cell properties of colorectal cancer cells which may be essential in treatment and prevention of relapse of this resistant cancer.

Acknowlegments: We thank Dr. Snorri Thorgeirsson for helpful comments about improving the manuscript. We also acknowledge the valuable advice and support of Drs Elizabeth Conner and Valentina Factor as well as the outstanding support of the Geneva Foundation, Tacoma, WA. We gratefully acknowledge the support provided by the Center for Cancer Research of the NCI for Project ZIA BC 011199 and by the Department of Defense for Grant Number W81XWH-11-1-0327. The opinions expressed in this manuscript are those of the authors and do not necessarily represent those of the National Cancer Institute, the National Institutes of Health, the Department of Health and Human Services or the Department of the Army.

References:

1. Kaufmann SH, Earnshaw WC. Induction of apoptosis by cancer chemotherapy. Exp Cell Res 2000;256:42-9.

2. Hayward RL, Macpherson JS, Cummings J, Monia BP, Smyth JF, Jodrell DI. Antisense Bcl-xl down-regulation switches the response to topoisomerase I inhibition from senescence to apoptosis in colorectal cancer cells, enhancing global cytotoxicity. Clin Cancer Res. 2003;9:2856-65.

3. Okumura K, Huang S, Sinicrope FA. Induction of Noxa sensitizes human colorectal cancer cells expressing Mcl-1 to the small-molecule Bcl-2/Bcl-xL inhibitor, ABT-737. Clin Cancer Res. 2008;14:8132-42.

4. Violette S, Poulain L, Dussaulx E, Pepin D, Faussat AM, Chambaz J, et al. Resistance of colon cancer cells to long-term 5-fluorouracil exposure is correlated to the relative level of Bcl-2 and Bcl-X(L) in addition to Bax and p53 status. Int J Cancer. 2002;98:498-504.

5. Schulze-Bergkamen H, Ehrenberg R, Hickmann L, Vick B, Urbanik T, Schimanski CC, et al. Bcl-x(L) and Myeloid cell leukaemia-1 contribute to apoptosis resistance of colorectal cancer cells. World J Gastro. 2008;14:3829-40.

6. Peddaboina C, Jupiter D, Fletcher S, Yap JL, Rai A, Tobin RP, et al. The downregulation of Mcl-1 via USP9X inhibition sensitizes solid tumors to Bcl-xl inhibition. BMC cancer. 2012;12:541.

7. Youle RJ, Strasser A. The BCL-2 protein family: opposing activities that mediate cell death. Nat Rev Mol Cell Biol. 2008;9:47-59.

8. Chen L, Willis SN, Wei A, Smith BJ, Fletcher JI, Hinds MG, et al. Differential targeting of prosurvival Bcl-2 proteins by their BH3-only ligands allows complementary apoptotic function. Mol Cell. 2005;17:393-403.

9. Certo M, Del Gaizo Moore V, Nishino M, Wei G, Korsmeyer S, Armstrong SA, et al. Mitochondria primed by death signals determine cellular addiction to antiapoptotic BCL-2 family members. Cancer cell. 2006;9:351-65.

10. Tahir SK, Yang X, Anderson MG, Morgan-Lappe SE, Sarthy AV, Chen J, et al. Influence of Bcl-2 family members on the cellular response of small-cell lung cancer cell lines to ABT-737. Cancer Res. 2007;67:1176-83.

11. Souers AJ, Leverson JD, Boghaert ER, Ackler SL, Catron ND, Chen J, et al. ABT-199, a potent and selective BCL-2 inhibitor, achieves antitumor activity while sparing platelets. Nature Med. 2013;19:202-8.

12. Raats DA, de Bruijn MT, Steller EJ, Emmink BL, Borel-Rinkes IH, Kranenburg O. Synergistic killing of colorectal cancer cells by oxaliplatin and ABT-737. Cell Oncol (Dordr). 2011;34:307-13.

13. Davids MS, Letai A, Brown JR. Overcoming stroma-mediated treatment resistance in chronic lymphocytic leukemia through BCL-2 inhibition. Leuk Lymp. 2013;54:1823-5.

14. Touzeau C, Dousset C, Le Gouill S, Sampath D, Leverson JD, Souers AJ, et al. The Bcl-2 specific BH3 mimetic ABT-199: a promising targeted therapy for t(11;14) multiple myeloma. Leukemia. 2013.

15. Vaillant F, Merino D, Lee L, Breslin K, Pal B, Ritchie ME, et al. Targeting BCL-2 with the BH3 mimetic ABT-199 in estrogen receptor-positive breast cancer. Cancer cell. 2013;24:120-9.

16. Mattoo AR, FitzGerald DJ. Combination treatments with ABT-263 and an immunotoxin produce synergistic killing of ABT-263-resistant small cell lung cancer cell lines. Int J Cancer. 2013;132:978-87.

17. Xu H, Krystal GW. Actinomycin D decreases Mcl-1 expression and acts synergistically with ABT-737 against small cell lung cancer cell lines. Clin Cancer Res. 2010;16:4392-400.

18. Brunelle JK, Ryan J, Yecies D, Opferman JT, Letai A. MCL-1-dependent leukemia cells are more sensitive to chemotherapy than BCL-2-dependent counterparts. Journal Cell Biol. 2009;187:429-42.

19. Letai A. Restoring cancer's death sentence. Cancer cell. 2006;10:343-5.

20. Chambers I, Colby D, Robertson M, Nichols J, Lee S, Tweedie S, et al. Functional expression cloning of Nanog, a pluripotency sustaining factor in embryonic stem cells. Cell. 2003;113:643-55.

21. Mitsui K, Tokuzawa Y, Itoh H, Segawa K, Murakami M, Takahashi K, et al. The homeoprotein Nanog is required for maintenance of pluripotency in mouse epiblast and ES cells. Cell. 2003;113:631-42.

22. Jeter CR, Badeaux M, Choy G, Chandra D, Patrawala L, Liu C, et al. Functional evidence that the self-renewal gene NANOG regulates human tumor development. Stem Cells. 2009;27:993-1005.

23. Jeter CR, Liu B, Liu X, Chen X, Liu C, Calhoun-Davis T, et al. NANOG promotes cancer stem cell characteristics and prostate cancer resistance to androgen deprivation. Oncogene. 2011;30:3833-45.

24. Palla AR, Piazzolla D, Abad M, Li H, Dominguez O, Schonthaler HB, et al. Reprogramming activity of NANOGP8, a NANOG family member widely expressed in cancer. Oncogene. 2013; Jun 10. doi: 10.1038/onc.2013.196. [Epub ahead of print]

25. Zbinden M, Duquet A, Lorente-Trigos A, Ngwabyt SN, Borges I, Ruiz i Altaba A. NANOG regulates glioma stem cells and is essential in vivo acting in a cross-functional network with GLI1 and p53. EMBO J. 2010;29:2659-74.

26. Zhang J, Espinoza LA, Kinders RJ, Lawrence SM, Pfister TD, Zhou M, et al. NANOG modulates stemness in human colorectal cancer. Oncogene. 2013;32:4397-405.

27. Noh KH, Kim BW, Song KH, Cho H, Lee YH, Kim JH, et al. Nanog signaling in cancer promotes stem-like phenotype and immune evasion. J Clin Invest. 2012;122:4077-93.

28. Samara RN, Laguinge LM, Jessup JM. Carcinoembryonic antigen inhibits anoikis in colorectal carcinoma cells by interfering with TRAIL-R2 (DR5) signaling. Cancer Res. 2007;67:4774-82.

29. Cao J, Li L, Chen C, Lv C, Meng F, Zeng L, et al. RNA interference-mediated silencing of NANOG leads to reduced proliferation and self-renewal, cell cycle arrest and apoptosis in T-cell acute lymphoblastic leukemia cells via the p53 signaling pathway. Leukemia Res. 2013;37:1170-7.

30. Yamaguchi S, Kurimoto K, Yabuta Y, Sasaki H, Nakatsuji N, Saitou M, et al. Conditional knockdown of Nanog induces apoptotic cell death in mouse migrating primordial germ cells. Development. 2009;136:4011-20.

31. Munshi A, Hobbs M, Meyn RE. Clonogenic cell survival assay. Methods Mol Med. 2005;110:21-8.

32. Ni Chonghaile T, Letai A. Mimicking the BH3 domain to kill cancer cells. Oncogene. 2008;27 Suppl 1:S149-57.

33. Boyer LA, Lee TI, Cole MF, Johnstone SE, Levine SS, Zucker JP, et al. Core transcriptional regulatory circuitry in human embryonic stem cells. Cell. 2005;122:947-56.

34. Yeung TM, Gandhi SC, Wilding JL, Muschel R, Bodmer WF. Cancer stem cells from colorectal cancer-derived cell lines. Proc Natl Acad Sci. 2010;107:3722-7.

35. Ma Y, Liang D, Liu J, Wen JG, Servoll E, Waaler G, et al. SHBG is an important factor in stemness induction of cells by DHT in vitro and associated with poor clinical features of prostate carcinomas. PloS One. 2013;8:e70558.

36. Zhang Z, Zhou Y, Qian H, Shao G, Lu X, Chen Q, et al. Stemness and inducing differentiation of small cell lung cancer NCI-H446 cells. Cell Death Dis. 2013;4:e633.

37. Fedr R, Pernicova Z, Slabakova E, Strakova N, Bouchal J, Grepl M, et al. Automatic cell cloning assay for determining the clonogenic capacity of cancer and cancer stem-like cells. Cytometry Part A. 2013;83:472-82.

38. Ibrahim EE, Babaei-Jadidi R, Saadeddin A, Spencer-Dene B, Hossaini S, Abuzinadah M, et al. Embryonic NANOG activity defines colorectal cancer stem cells and modulates through AP1- and TCF-dependent mechanisms. Stem Cells. 2012;30:2076-87.

39. Goff DJ, Recart AC, Sadarangani A, Chun HJ, Barrett CL, Krajewska M, et al. A Pan-BCL2 inhibitor renders bone-marrow-resident human leukemia stem cells sensitive to tyrosine kinase inhibition. Cell stem cell. 2013;12:316-28.

40. Lagadinou ED, Sach A, Callahan K, Rossi RM, Neering SJ, Minhajuddin M, et al. BCL-2 inhibition targets oxidative phosphorylation and selectively eradicates quiescent human leukemia stem cells. Cell stem cell. 2013;12:329-41.

Figure Legends

Figure 1: Antitumor effects of LVNG1/LVNp81-ABT-737 combinations. Three million parental LS174T cells or LS174T cells transduced with LV shNEG, shNG-1 or shNp8-1 were injected subcutaneously into groups of 8 NOD/SCID male mice. At Day 8 ABT-737 (100 mg/ml) was injected daily intraperitoneally for 5 days. Panel A) three mice from each group were sacrificed on the 8th day before ABT-737 treatment, tumors collected and qRT-PCR performed to determine the relative expression of total transcripts of the *NANOGs.* Mean ± SD of the expression of the *NANOGs* normalized by *GAPDH.* Panel B) Mean growth curves of each group of mice. Panel C) Box and whisker plots for each group of mice with Mean and 5% - 95% confidence intervals presented by the error bars. The P values were determined by one-way ANOVA and compared to the Control (Untreated) group.

Figure 2: Dose response of CRC cell lines to the BH3 mimetic ABT-737. Panels A -C) Clone A, CX-1 or LS174T cells were treated with ABT-737 (0.2 to 60uM) for 72 hrs. Cell survival was determined using the WST-1 reagent. The viability of cells (% of Control) is presented as % absorbance of treated cells at 450nm/% absorbance of untreated cells at 450nm expressed as a percent of the untreated parental cells. IC50's were calculated with GraphPad Prism 6 using the nonlinear regression subprogram. Panel D) Immunoblot analysis for detection of MCL-1, BCL-2, BCl- xL, BCL-W, and BIM levels in Clone A, CX-1 and LS174T.

Figure 3: ABT-737 and LV shRNA Combination Therapy Increases Inhibition of CRC Growth. 5,000 CRC cells were cultured in monolayer culture in individual wells of a 96 well microtiter plate in complete medium and LV shRNA or ABT-737 or both added as indicated for a total of 8 days. Cells were treated with either LV shRNA for 5 days or 1 μM ABT-737 for 3 days or with both from the beginning of the culture. The "None" cells did not receive any ABT-737 whereas the "ABT First", ABT Second" or ABT Continuous" represent cells exposed to ABT-737 first and then LV, or "ABT Second" with cells exposed to LV shRNA first for 5 days and then ABT-737 for 3 days or "ABT Continuous" where both agents were added at the beginning of the 8 day culture. Results are presented as Means with SD. P values are the significance of the indicated LV shNG-1 and/or shNp8-1 compared to the LV shNEG in the same treatment group determined by 2-

way ANOVA. Where there is a horizontal cupped bracket spanning across shNG-1 and shNp8-1, the P value of each compared to the corresponding shNEG control is the indicated value.

Figure 4: LV shRNA to *Nanog* or *NanogP8* Inhibits MCL-1 and increases Caspase 3/7 Activity. Panel A) Clone A, CX-1 or LS174T cells were treated with the indicated LV shRNA for 5 days in monolayer culture or left untreated. Lysates were blotted and probed for NANOG and MCL-1 protein expression. Panel B) the three cell lines were treated with LV shRNA alone for 7 days or LVshRNA for 5 days followed by ABT-737 (1uM) for 2 days in triplicate in complete medium. Caspase 3/7 activity was determined in the wells using the Promega Caspase 3/7 –Glo kit according to the manufacturer's protocol. The results are Mean plus SD of the activity normalized to the untreated control cells within each experiment. P values are the significance of the indicated Caspase 3/7 fold increase in LV shNG-1+ABT-737(1uM) and shNp8-1 + ABT-737 (1uM) compared to the LV shNEG+ ABT-737(1uM) for each cell line determined by 1-way ANOVA with the Holm-Sidak multiple comparisons test. Panel C) Clone A or LS174T cells were cultured in complete medium for 16 hr and then treated with LV shNEG or shNp8-1, ABT-737 (2uM) or the combination. Four hours later, 10µM Caspase 3 inhibitor (Z-DEVD-FMK) was added. Cell viability was determined 5 days later. Results are presented as the Mean plus SD normalized to the untreated control cells. P values are determined by one-way ANOVA with means compared to the untreated cells with the Holm-Sidak multiple comparisons test.

Figure 5: Activity of ABT-199 in CRC cells alone or in combination with shRNA against *Nanog* and *NanogP8*: Panel A) Clone A, CX-1 and LS174T cells were treated with ABT-199 for 72 hrs and viability determined with IC_{50} calculated for each cell line as described in Figure 2. Panel B) 5,000 CRC cells were cultured in complete medium and LV or ABT-199 or both added as indicated for a total of 8 days. The scheme of the experiment was the same as described for Figure 3. Results are mean plus SD normalized to the untreated CRC cells. P values are the significance of the indicated LV shNG-1 and/or shNp8-1 compared to the LV shNEG in the same treatment group as determined by 2-way ANOVA with the Holm-Sidak multiple comparisons test.

Figure 6: Inhibition of *Mcl-1* expression is similar to the effect of LV shNG-1 or shNp8-1 on Caspase 3/7 activity when combined with BH3 mimetics: Panel A) Clone A, CX-1 or LS174T cells were transfected with siRNA to *Mcl-1* (siMCL-1, 100nM) or scrambled RNA (scRNA, 100nM) and lysed and immunoblotted for MCL-1 and ß-actin after 72hrs . Panel B) The three cell lines were transfected with siRNA *Mcl-1* (100nM) and 3 days later ABT-737 (2µM) or ABT-199 (2µM) were added as indicated. Caspase 3/7 activity was measured at a total of 5 days by Promegaspase 3/7 –Glo kit according to the manufacturer's protocol. The results are presented as Mean plus SD of the activity normalized to the untreated control cells within each experiment. P values were determined by one-way ANOVA with Holm-Sidak multiple comparisons correction test. Panel C) 5000 LS174T cells were seeded in individual wells of a 96 well plate in triplicate and next day treated with LVshNEG and LVshNP81. After 3 days, p-TOPO-MCL-1 was transfected using Lipofectamine. After 48 hrs, 4 µM ABT-737 was added and cell viability was measured 3 days later by WST-1 metabolism . The viability of cells is represented as Mean + SD of the % absorbance of cells at 450nM compared to the controls. P values were calculated by 1-way ANOVA. Panel D) Lysates of the combinations of ABT-737 and LV shRNAs on the MCL-1 and ß Actin protein expression in LS174T cells treated as in Panel C) were probed and demonstrate MCL-1 is overexpressed in all of the p-TOPO MCL-1 tranfected cells.

Supplementary Figure Legends:

Figure S1: Dose response curve of CX-1 cells treated with LVshNp81 in combination of increasing concentrations of ABT-737: 5000 CX-1 cells were seeded in triplicate in 96 well plates and next day treated with LVshNp8-1 alone or in combination with increasing concentrations of ABT-737 (0.2µM to 12.8 MM). Cell viability was measured after 5 days by WST-1 assay. Viable cells (% of Control) is % absorbance of treated cells at 450nM/ % absorbance of untreated control cells at 450nM expressed as a percentage. The data were analyzed in GraphPad Prismv6 using the non-linear dose response curve fit program. P value was calculated by t Test on the IC_{50}'s.

Figure S2:Lentiviral Delivered (LV) shRNA to *NANOG* or *NANOGP8* decreases the phosphorylation of AKT and decreases MCL-1 levels: LS174T cells were treated with the

indicated LV shRNA for 5 days in monolayer culture and the Mean ± SD of the relative expression of total NANOG transcripts (Panel A) and MCL-1 (Panel B) are presented. Expression was normalized by GAPDH expression. Lysates of Clone A cells were probed for AKT, pAKT-Ser473, NANOG and MCL-1 protein with ß actin as a control (Panel C).

Figure S3: Re-plating assay of CRC cells treated with LV shRNA against NANOG and NANOGP8 and ABT-737: Clone A ,CX-1 and LS174T cells were treated with the combination of LV shRNA and ABT-737 and re-plated in 60 mm dishes in duplicates as described in Materials and Methods. P values were determined by 2-way ANOVA corrected for multiple comparisons against ABT-737 alone. The combination of LVshNp8-1 and ABT-737 reduces the re-growth capacity all the three cell lines when they are replated in complete medium in monolayer.

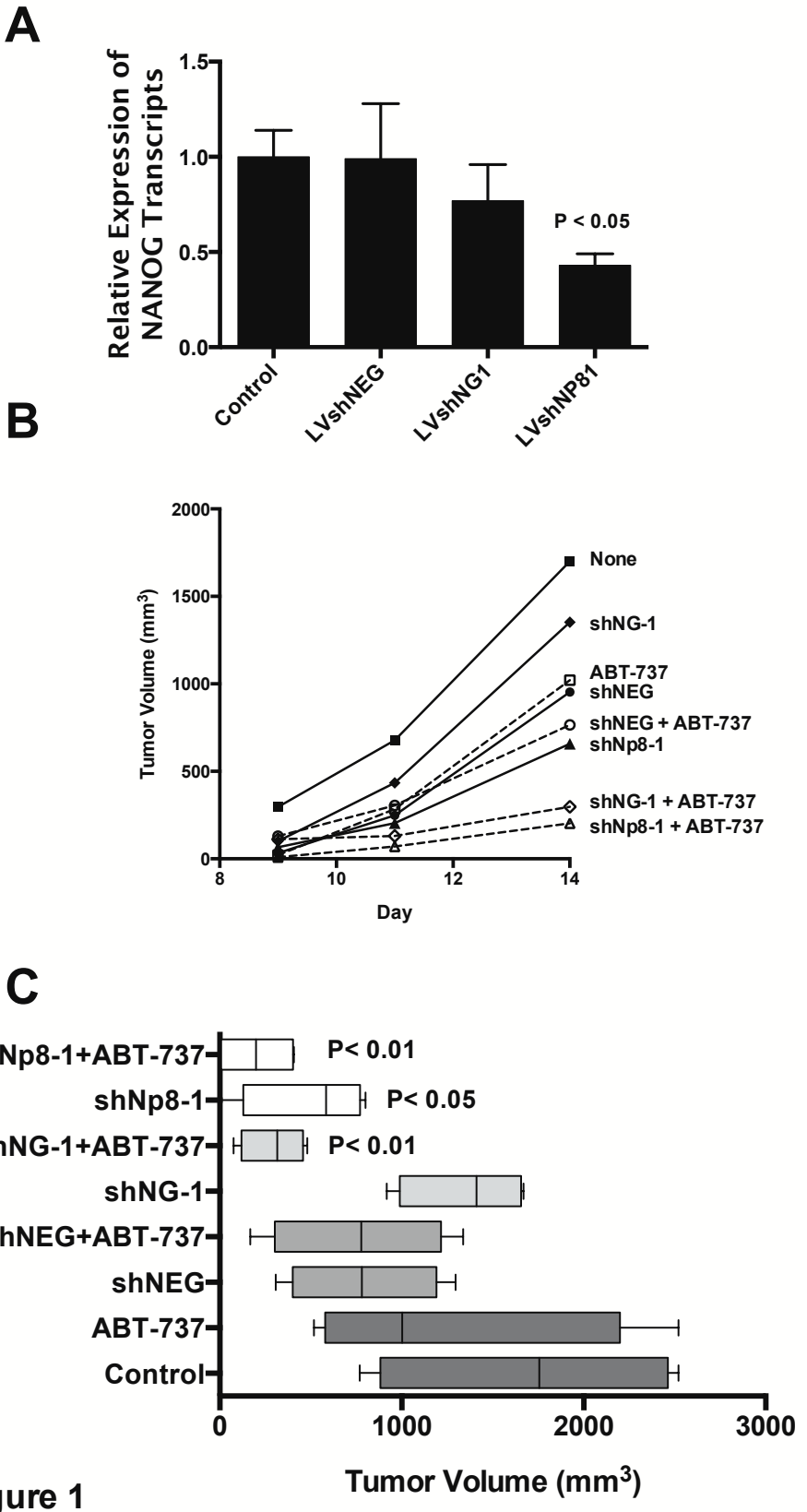
A
Relative Expression of NANOG Transcripts
1.5
1.0
0.5
0.0
P < 0.05
Control
LVshNEG
LVshNG1
LVshNP81
B
Tumor Volume (mm3)
2000
1500
1000
500
0
8
10
12
14
Day
None
shNG-1
ABT-737
shNEG
shNEG + ABT-737
shNp8-1
shNG-1 + ABT-737
shNp8-1 + ABT-737
C
shNp8-1+ABT-737
shNp8-1
shNG-1+ABT-737
shNG-1
shNEG+ABT-737
shNEG
ABT-737
Control
P< 0.01
P< 0.05
P< 0.01
0
1000
2000
3000
Tumor Volume (mm3)

Figure 1

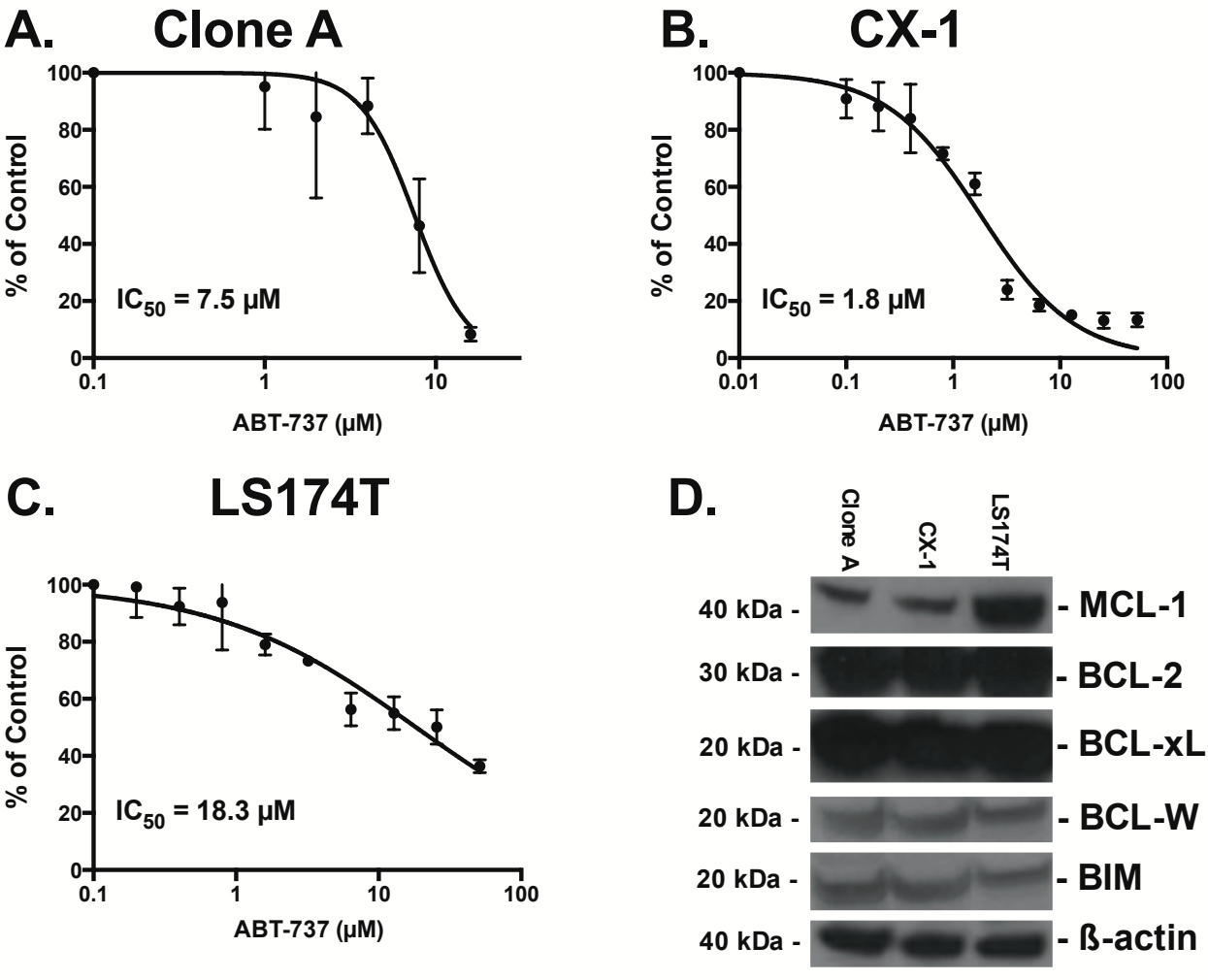
A.
Clone A
% of Control
IC50 = 7.5 µM
ABT-737 (µM)
B.
CX-1
% of Control
IC50 = 1.8 µM
ABT-737 (µM)
C.
LS174T
% of Control
IC50 = 18.3 µM
ABT-737 (µM)
D.
Clone A
CX-1
LS174T
40 kDa - MCL-1
30 kDa - BCL-2
20 kDa - BCL-xL
20 kDa - BCL-W
20 kDa - BIM
40 kDa - ß-actin

Figure 2

A. Clone A

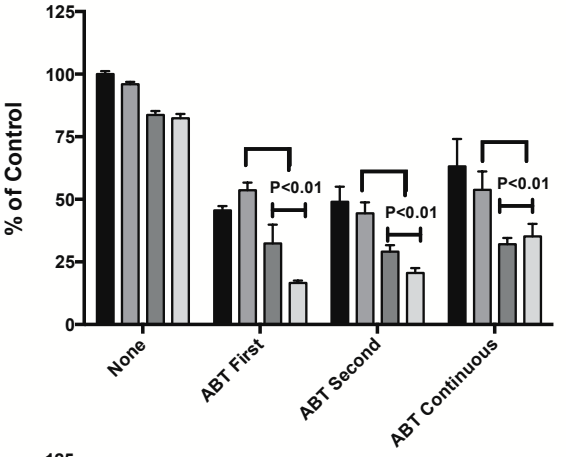

B. CX-1

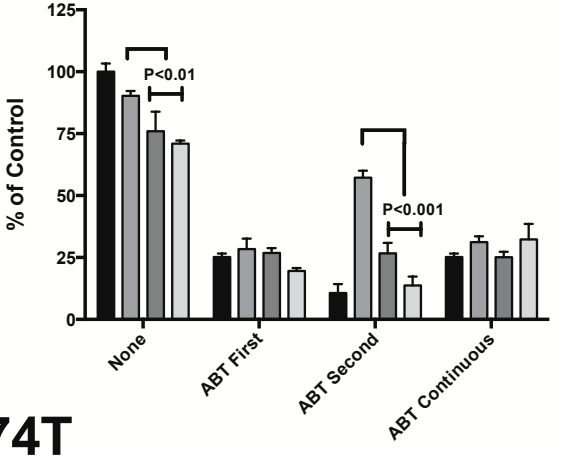

C. LS174T

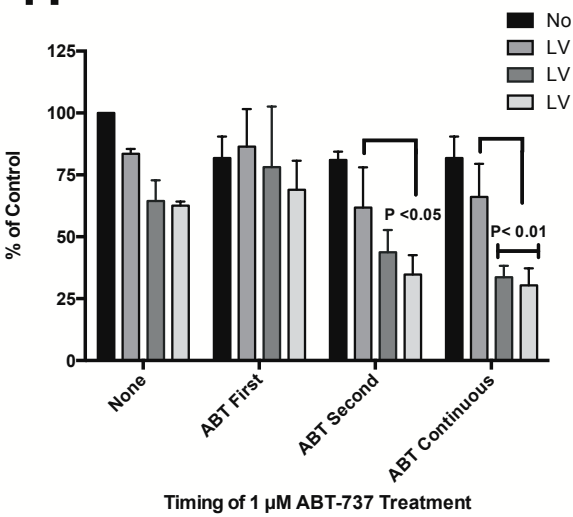

Figure 3

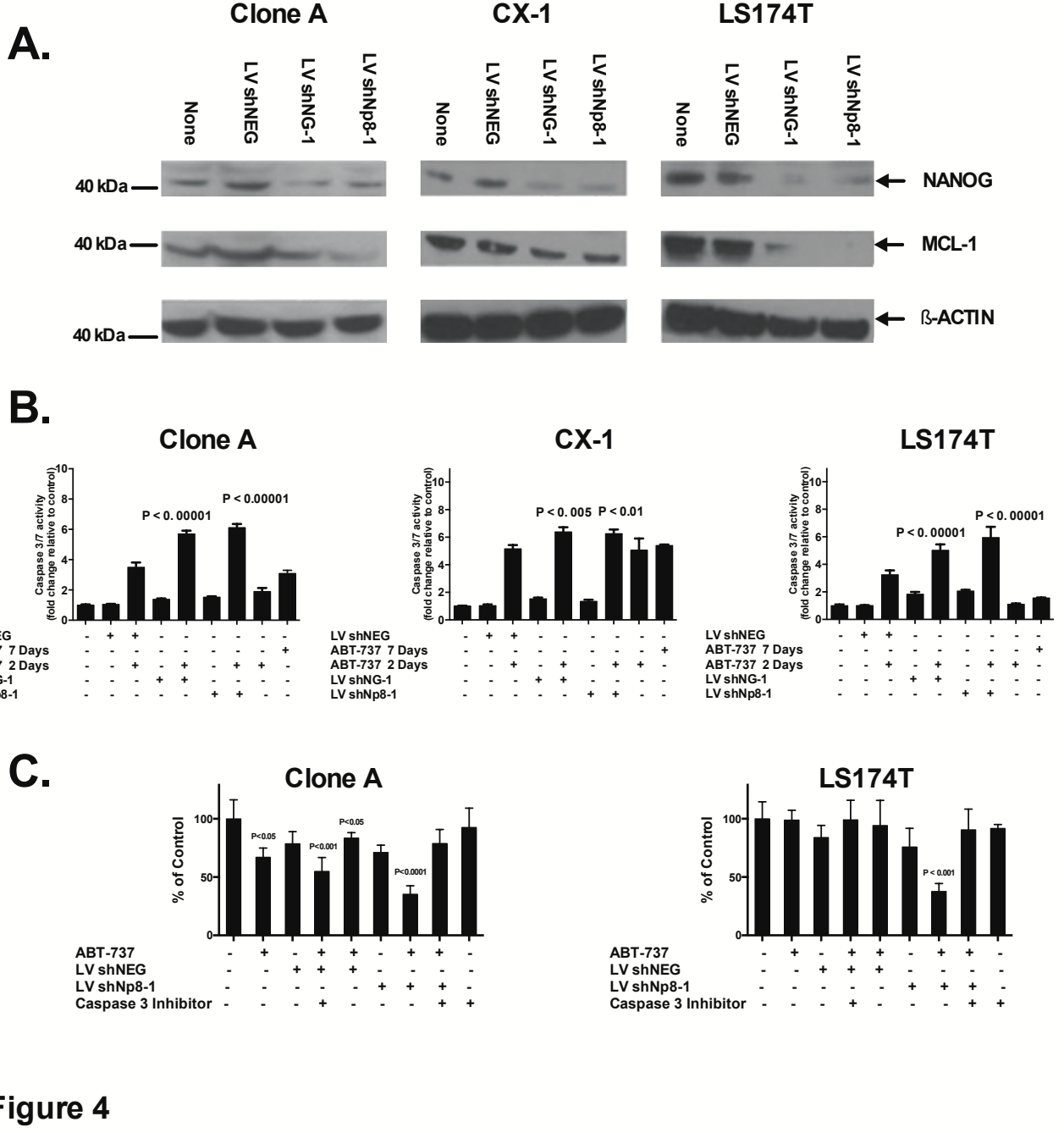
A.
Clone A
CX-1
LS174T
None
LV shNEG
LV shNG-1
LV shNp8-1
40 kDa
NANOG
MCL-1
ß-ACTIN
B.
Clone A
CX-1
LS174T
Caspase 3/7 activity (fold change relative to control)
P < 0. 00001
P < 0.00001
P < 0. 005
P < 0.01
LV shNEG
ABT-737 7 Days
ABT-737 2 Days
LV shNG-1
LV shNp8-1
C.
Clone A
LS174T
% of Control
P<0.05
P<0.001
P<0.05
P<0.0001
P < 0.001
ABT-737
LV shNEG
LV shNp8-1
Caspase 3 Inhibitor

Figure 4

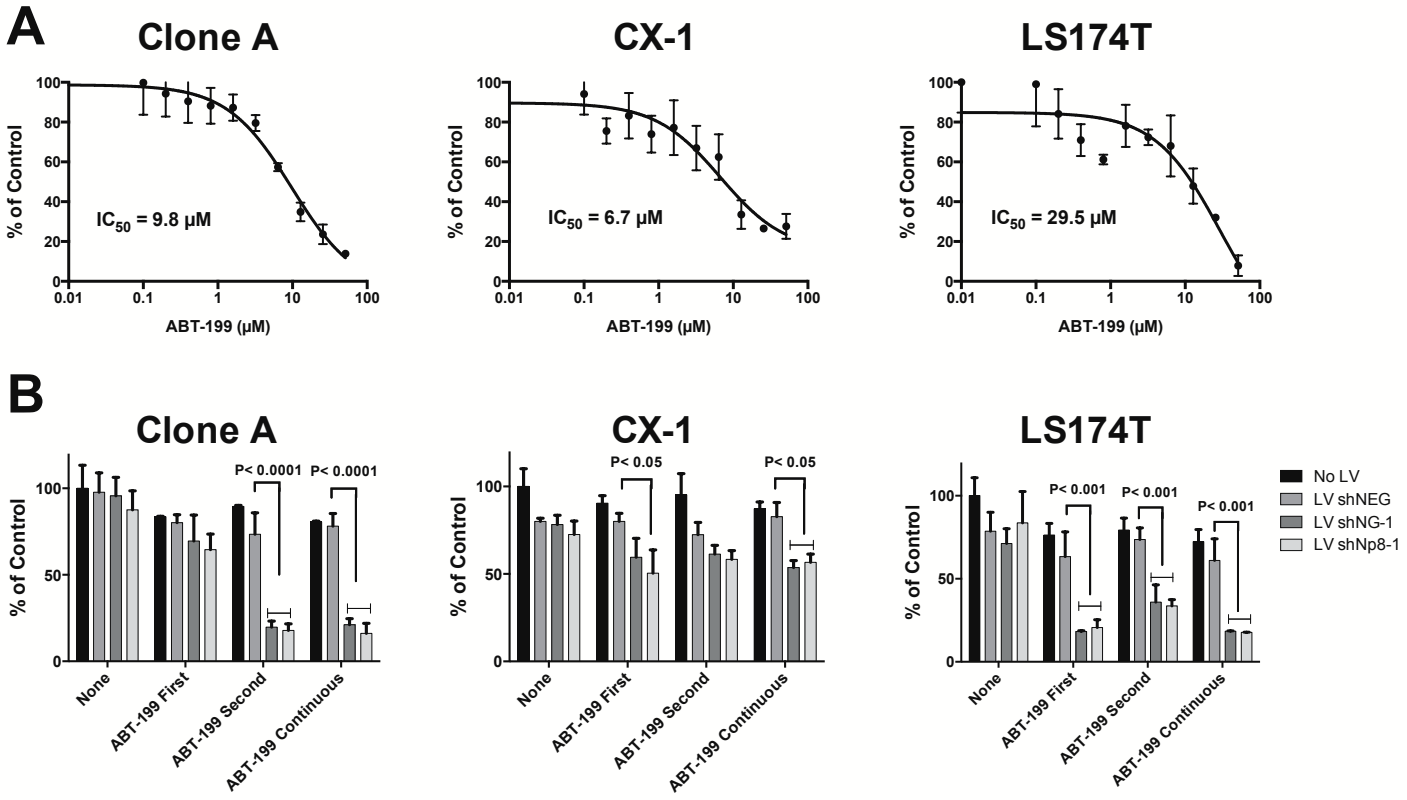
A
Clone A
CX-1
LS174T
% of Control
IC50 = 9.8 μM
IC50 = 6.7 μM
IC50 = 29.5 μM
ABT-199 (μM)
B
P< 0.0001
P< 0.05
P< 0.001
None
ABT-199 First
ABT-199 Second
ABT-199 Continuous
No LV
LV shNEG
LV shNG-1
LV shNp8-1

Figure 5

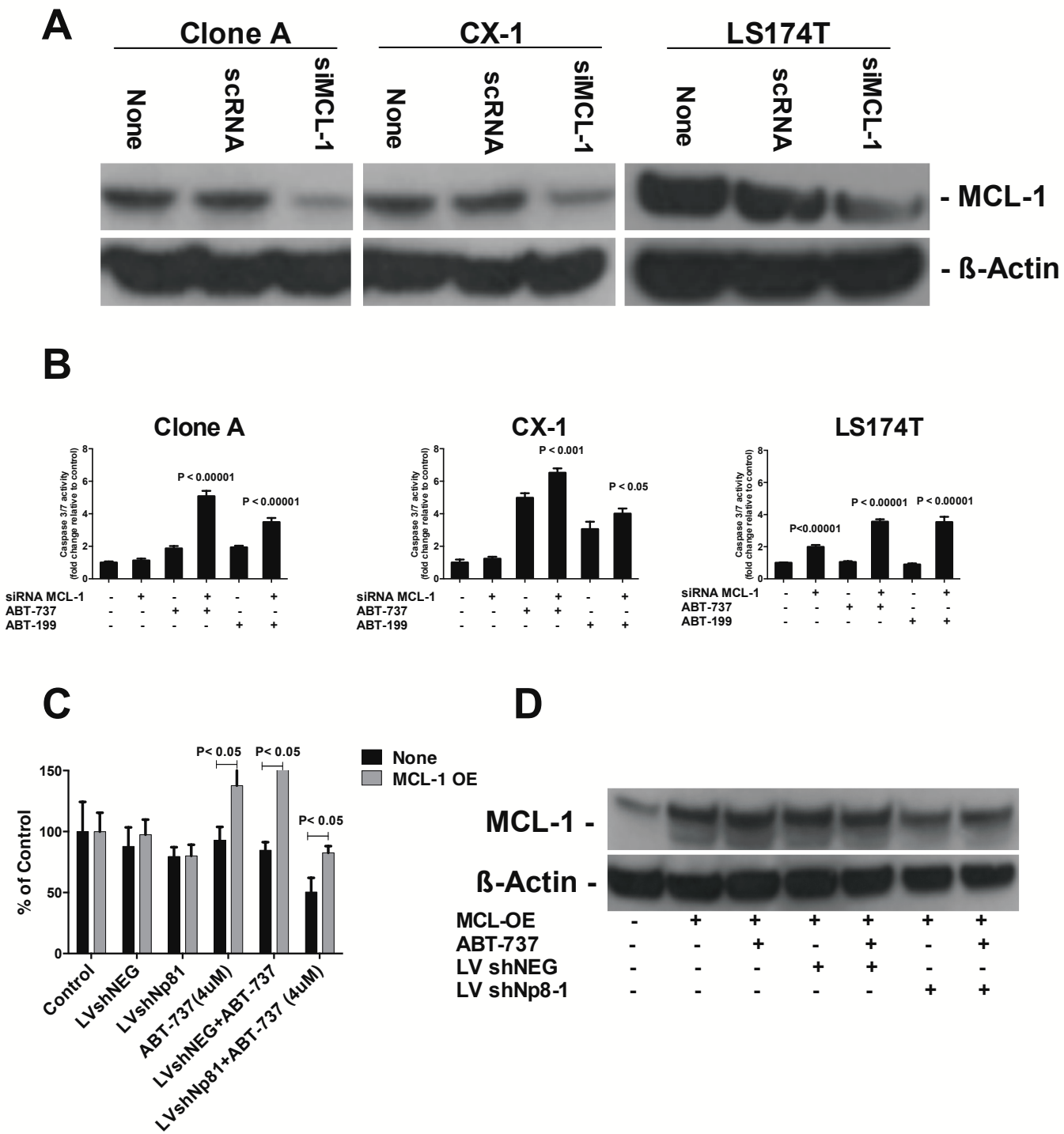
A
Clone A
CX-1
LS174T
None
scRNA
siMCL-1
- MCL-1
- ß-Actin
B
Clone A
CX-1
LS174T
Caspase 3/7 activity (fold change relative to control)
P < 0.00001
P < 0.00001
P < 0.001
P < 0.05
P<0.00001
P < 0.00001
P < 0.00001
siRNA MCL-1
ABT-737
ABT-199
C
D
None
MCL-1 OE
% of Control
P< 0.05
P< 0.05
P< 0.05
Control
LVshNEG
LVshNp81
ABT-737(4uM)
LVshNEG+ABT-737
LVshNp81+ABT-737 (4uM)
MCL-1 -
ß-Actin -
MCL-OE
ABT-737
LV shNEG
LV shNp8-1

Figure 6

Allelotypic Inhibition of Embryonic Transcription Factor Decreases Three-Dimensional Growth of Colorectal Carcinoma

Abid R. Mattoo*[1], Jingyu Zhang*[1], Luis A. Espinoza[1], Nikolay Korokhov[1], J. Milburn Jessup[1,2,3]

[1]Laboratory of Experimental Carcinogenesis
Center for Cancer Research
National Cancer Institute

[2]Cancer Diagnosis Program
Division of Cancer Treatment and Diagnosi
National Cancer Institute

[3]Point of Contact: J. Milburn Jessup, MD

9609 Medical Center Drive – Room 4W410

Bethesda, MD, 20892-7430

*These 2 authors contributed equally to this work.

The authors with the exception of NK are employees of the Federal Government and declare that they do not have financial conflicts of interest. NK also does not have any conflict of interest as an employee of the Geneva Foundation.

Running Title: *NANOG* Inhibition Enhances Apoptosis

Keywords: Suspension Culture, 3-D Growth, Lentiviral shRNA, NANOG, NANOGP8, caspase-dependent apoptosis

Abbreviations: 3-D – three-dimensional, CRC – colorectal carcinoma, EdU- 5-ethynyl-2'-deoxyuridine, GFP- Green Fluorescent Protein, LV- Lentiviral or Lentivirus Vector, MOI – Multiplicity of Infection, qRT-PCR – quantitative reverse transcriptase-polyemerase chain reaction, SFM – serum-free medium, shNp-1 and shNG-1 – shRNA to NANOGP8 or NANOG, respectively (allelotypic shRNA targeting codon 759), shNEG – a control shRNA, SNP – single nucleotide polymorphism, TUNEL - Terminal deoxynucleotidyl transferase dUTP nick end labeling, VSV-G - Vesicular stomatitis virus G protein

Abstract: 202 words

Manuscript: 4,248 words

7 Figures, 2 in color

Supplemental Information: 2 Figures, 1 Table plus STR certification of cells

Pages: 29

ABSTRACT

Inhibition of *NANOG* and its retrogene *NANOGP8* decreases pluripotency and self-renewal in human carcinomas, sarcomas and leukemias with *NANOGP8* being the prevalent isoform expressed in human malignancies. The major difference between the two genes is a single nucleotide variant: c.759G>C, p.Gln253His. We postulated that allelotypic shRNAs targeting codon 759 would increase caspase-dependent apoptosis in human colorectal carcinomas (CRC) growing in three-dimensions (3-D). Lentiviral (LV) allelotypic shRNA to *NANOGP8* (shNp8-1) or *NANOG* (shNG-1) inhibited growth *in vivo* and *in vitro* compared to CRC treated with a control shRNA (shNEG) or left untreated. CRC cells transduced with LV shNp8-1 or shNG-1 at low multiplicity of infection reduced total *NANOG* transcripts and inhibited CRC suspension culture growth by 45- 50% within 3 days, but shNEG transduction did not. Overexpression of *NANOGP8* or *NANOG* increased 3-D growth. Allelotypic shRNA did not inhibit proliferation in suspension culture, but activated caspase 3 and 9 activity and caspase 3 and 9 peptide inhibitors stimulated CRC growth. Allelotypic shRNA transduction also significantly decreased regrowth potential in a colony-forming assay.

Implication: Inhibition of *NANOGP8* or *NANOG* by allelotypic shRNA induces caspase-dependent apoptosis during 3-D growth that may be useful in increasing the efficacy of clinical treatments that depend on caspase-dependent apoptosis.

Introduction:

Transition from two-dimensional monolayer to three-dimensional (3-D) suspension cultures provides models of tumors that may be molecularly more closely associated with malignant tumors growing in vivo (1-3). 3-D cultures in serum-free medium have been used to isolate cancer stem cells (4-7) while 3-D cultures in semi-solid media have provided insights into not only developmental pathways (review see Yamada and Cukierman, 3), but also why tumors are more resistant to therapy in 3-D culture (8, 9) and in vivo (10-13). Malignant cells attached to a substrate in monolayer form 3-D spheroids in aqueous or semi-solid cultures (14). In addition, 3-D cultures without stromal elements also undergo anoikis, a form of apoptosis caused by loss of cell adhesion to substrates (15). In human colorectal carcinoma (CRC) cells anoikis involves the clustering of TNFRSF10B (TRAIL receptor 2 or DR5) into death signaling clusters that activate caspase 8 and the extrinsic pathway of apoptosis with little activation of caspase 9 and the mitochondrial or intrinsic pathway of apoptosis (16). Thus, 3-D suspension cultures may provide a model for tumor growth that better mimics the balance between survival and death from apoptosis in tumors.

We (17) have demonstrated that *NANOGP8*, a retrogene of *NANOG*, can substitute for NANOG in directly promoting stemness in CRC as measured by the ability of individual CRC cells to form spheroids. These data extended those of Jeter et al (18) who demonstrated that *NANOGP8* may replace *NANOG* to stimulate proliferation in monolayer culture. In addition, *NANOG* expression is associated with the stage and prognosis of cervical cancer and regulates tumorigenicity and immune resistance of various tumor cells through regulation of the antiapoptotic Bcl-2 family protein Mcl-1 (19). *NANOG* is a stem cell transcription factor that is essential for embryonic development, reprogramming normal adult cells and malignant transformation and progression. *Nanog* deficient mice fail to develop beyond the blastocyst stage (20). Conditional knockdown studies revealed that deficiency of *Nanog* results in the apoptotic death of mouse migrating primodial germ cells (21). Knockdown of other embryonic stem transcription factors such as *Oct4* in murine embryonic stem cells also enhances apoptosis induced by stress factors such as etoposide, UV or heat shock through the Stat 3/survivin

pathway (22). In addition, Zhang et al (17) demonstrated that *NANOG* and *NANOGP8* transcript levels increased in spheroids compared to monolayer cultures. This suggests that expression of the *NANOGs* is sensitive to 3-D growth signals and/or that *NANOG* expression increases as an anti-apoptotic factor when malignant cells are exposed to apoptotic stress. Thus, inhibition of *NANOG* or *NANOGP8* may enhance apoptosis when CRC cells are exposed to apoptotic stress.

In the current study we postulated that transduction of Lentivirus (LV) delivered shRNA targeting a SNP in *NANOGP8* or *NANOG* in CRC inhibits growth of CRC aggregates and spheroids in 3D-culture *in vitro* or *in vivo*. *NANOG* and *NANOGP8* differ only in 5 nucleotides and 2 amino acids in the coding sequence with the important non-synomonous variant c.759G > C, p.Gln253His (23, 24). shRNAs were designed to target the two variants at codon 759 to create allelotypic shRNAs for *NANOG* and *NANOGP8* (17). Transduction with either allelotypic LV shRNA induces apoptosis in CRC growing in 3-D in vitro or in vivo through a caspase-dependent pathway that involves the intrinsic pathway. Thus, targeting the *NANOGs* may inhibit growth of human CRC.

Materials and Methods

Reagents

Lipofectamine 2000 for transfections was purchased from Invitrogen Life Technologies (Grand Island, NY). Polybrene and protamine sulfate for Lentivirus transduction was purchased from Sigma-Aldrich (St. Louis, MO). Precast NU-PAGE 4–12 % Bis Tris gels, NU-PAGE MES SDS Running Buffer and NU-PAGE transfer buffer were purchased from Invitrogen Life TechnologiesSingle cell profiling for caspases 3 (PhiPhiLux), 8 (CaspaLux), and 9 (CaspaLux) were obtained from OncoImmunin (Gaithersburg, MD). Caspase 3, 8 and 9 inhibitors were obtained from R & D Systems (Minneapolis, MN) as was polyclonal goat anti-human NANOG (AF1997). Allelotypic shRNAs were shNg-1 to NANOG (target sequence 5'-CUGCAUGCAGUUCCAGCCA-3'), shNp8-1 to NANOGP8 (target sequence 5'-CUGCAUGCACUUCCAGCCA-3') with the control vector shNEG (target sequence 5'-UAGCGACUAAACACAUCAA-3') and created in LV as described in Zhang et al (17).

Cell culture, cell transfection, lentivirus packaging and cell transduction

Clone A is a subclone of the DLD-1 cell line (25). CX-1 is a highly metastatic variant of HT29 (26) and LS174T is a CRC cell line obtained from ATCC and used in our previous study (27). MIP-101 is a poorly differentiated CRC line derived from ascites (28). KM-12c is a weakly metastatic CRC that is a member of the NCI-60 panel (29). All cell lines were cultured in RPMI 1640 (Invitrogen) media supplemented with 10% fetal bovine serum (Invitrogen) and 2mM L-glutamine (Invitrogen) at 37°C, 5% CO_2 incubator. The Lentivirus particles containing the allele specific shRNA's for *NANOG* (shNg-1), *NANOGP8* (shNp8-1) and negative control (shNEG) were produced by co-transfection of 293T cells with packaging and envelope plasmids using Lipofectamine 2000 (Invitrogen) as described (17). The transduction of the lentiviral particles at an MOI of 5-8 for all the experiments was done using polybrene or protamine sulfate (Sigma-Aldrich, St. Louis, MO) as the transducing agent.

Assays:

The suspension culture was performed as described (17) with the modification that 2000 cells were plated in ULLA 96 well microtiter plates (Cat # 3474, Corning Life Sciences,

Corning, NY) in triplicate in serum-free medium (SFM) (Neuroccult A, Stem Cell Technologies, Vancouver, BC, CA). After 24 hr cells were treated with LV shNEG, LVshNG-1 and LVshNp8-1 in SFM and incubated for a further 3 days at Multiplicity of Infection (MOI) or 5 - 10. Individual wells were imaged with a 2x Objective on a Nikon TE2000-U Inverted microscope and tumor areas analyzed with ImageJ (NIH, Bethesda, MD). In addition, CRC cells transfected with *Luc2* plasmid (pGL4.50[luc2/CMV/Hygro] Vector, EU921840, Promega Corp., Madison, WI) were collected and then analyzed with the Luciferease Assay System (Cat # E1500, Promega Corp) according to the manufacturer's instructions. For the regrowth assay surviving cells at the end of the suspension culture were harvested and 500 cells seeded in 35 mm diameter Petri dishes (Corning, Tewksbury MA, USA) in RPMI-1640 media with supplements. The cells were incubated for 14 days and fixed and stained with 0.05 % Crystal violet in 10% neutral-buffered formalin (37% vol), methanol (1%) and 0.15 M PBS (62% vol). The plates were thoroughly washed with water and colonies were counted. Single Cell Profiling for caspase activity was performed by post-labeling suspension cultures with the individual caspase fluorescent dyes according to the manufacturer's instructions. TUNEL assays were performed as previously described after 96 hr of suspension culture (16). Cells were imaged and analyzed with ImageJ as previously described (16). For assessment of caspase function individual caspase 3, 8 or 9 inhibitors were added 2 hr after LV transduction at 10 μM and then cultures analyzed as above. qRT-PCR was performed as previously described (17). DNA labeling was performed with the EdU Click It kit (5-ethynyl-2'-deoxyuridine, Cat # C10339, Invitrogen, Grand Island, NY 14072) according to the manufacturer's protocol. EdU labeling was performed 72 hr after LV shRNA transduction.

Animal Experiments:

Intratumoral injection with LV shRNAs was performed under protocol LEC-052 approved by the NIH Animal Care and Use Committee. Seven week old male NOD/SCID mice produced by the Frederick Animal Production Facility were injected in the sub cutis with 1 X 10^6 viable CX-1 cells. Nine days later tumors were injected at a MOI of 1-3 LV when ~3-4 mm diameter into groups of 6 -14 mice. Tumor areas were calculated by the product of the 2 largest perpendicular diameters and results presented as the difference between the size of tumors present 8 days after intratumoral injection and just before injection.

Statistical Analysis:

ANOVA was performed for statistical analysis of multiple comparisons. Data in graphs are presented as mean ± S.D. except where indicated in the text. For the analyses, $P<0.05$ was considered to be statistically significant. All experiments were performed in triplicate and repeated independently. Analyses were performed in GraphPad Prism version 6.0a (GraphPad Software, Inc., La Jolla, CA).

Results

Intratumoral Lentiviral shRNA to *NANOGs* Inhibits Tumor Growth

Three to four mm diameter CX-1 tumors were injected with a 5 Multiplicity of Infection (MOI) of LV shNp8-1, shNG-1 or the control vector shNEG with tumors measured before and after intratumoral injection and the difference in areas calculated 8 days later (Figure 1A). The mean of the differential area of tumors injected with an allelotypic LV shRNA to either *NANOG* or *NANOGP8* was 31% smaller than that of the combined controls of mice injected with LV shNEG or left Untreated (mean of LV shRNAs to *NANOGs* was 26.4 ± 3.2 mm^2, N=25 versus 37.9 ± 4.3 mm^2, N=23, P= 0.03 by t test). These results suggested that treatment in vivo, even at low MOI, to reduce either *NANOGP8* or *NANOG* expression inhibited tumor growth. This experiment is a proof of principle that shRNA to the *NANOGs* may inhibit tumor growth although the number of LV viral particles to treat even small tumors was high (~50 viral particles = 1 MOI). As a result, further experiments were performed with CRC grown in vitro in 3-D aqueous suspension culture to determine the mechanism by which LV shRNA may decrease tumor survival and growth.

Growth of CRC in Suspension Culture Increases Both NANOG Protein Expression and Apoptosis While shRNA to *NANOGP8* Decreases Total Transcripts of the *NANOGs*.

We have previously demonstrated that transcripts of both *NANOG* and *NANOGP8* are increased in CRC growing in suspension compared to monolayer culture (17). We first assessed the expression of NANOG protein in the CX-1, MIP-101 and KM-12c cell lines cultured for 4 days in suspension culture and compared to the same cells cultured in monolayer. Since *NANOG* and *NANOGP8* only differ in 2 amino acids, antibodies to NANOG detect both proteins. Total *NANOG* protein expression increased 1.5- to 5-fold in these cell lines along with a commensurate increase in apoptosis measured by TUNEL staining (Supplemental Figure 1, Figure 1B and C). These results confirm that immunoreactive NANOG protein increases as *NANOG* and *NANOGP8* transcript levels increase in CRC cells growing in suspension as 3-D

constructs. These results also suggest that NANOG levels increase as CRC are undergoing anoikis.

CRC were transduced with LV shRNAs 24 hr after introduction to suspension culture and then analyzed for total *NANOG* transcript expression by qRT-PCR 72 hr later. Only LV to *NANOGP8* (shNp8-1) consistently decreased expression of *NANOG*-related transcripts in suspension cultures of Clone A, CX-1, and LS 174T compared to the LV shNEG control (Figure 1 D-F, respectively). Thus, suspension culture by itself increases the expression of *NANOG*-related transcripts and proteins. However, shRNA to *NANOGP8* successfully decreases total *NANOG*-related transcript expression by at least 50-90% depending on the cell line while shRNA to *NANOG* was less active.

Development of a 3-D Suspension Culture Assay for CRC Cells.

Two thousand CRC cells stably transfected with *Luc2* were cultured in SFM in individual wells of an Ultra Low Attachment (ULLA) 96 well microtiter plate. Sixteen hours later LV shRNA was added at a MOI of 5-10 infectious particles for each CRC cell originally plated. Aggregates and spheroids were imaged 3 days later under low (2x) magnification and tumor areas measured. LV delivered shNp8-1 inhibited the area of CX-1 cells by 45 to 66% compared to untreated CX-1 cells or CX-1 cells treated with LV shNEG or shNG-1 (Figure 2b, c). Luminescence results in the CX-1 cells in suspension were significantly associated with tumor area measurements (Figure 2c,d). We validated the utility of the optical measurements by demonstrating significant correlation between luminescence and tumor area in multiple experiments with Clone A and CX-1 (Figure 2e, f, respectively) and including untreated and all groups of LV treated cells. As a result, we used optical measurements of tumor area to assess further the effects of transduction with LV delivered shRNAs in CRC cells in 3-D culture.

LV shRNA Treatment Inhibits Growth of CRC Aggregates and Spheroids in Suspension Culture

We then tested whether LV shRNA transduction decreased the 3-D growth of 3 CRC lines. CRC cells transduced with LV shNp8-1 (shRNA to *NANOGP8*) were ~50% smaller than either untreated CX-1 cells or CX-1 cells transduced with LV shNeg, the negative control vector (Figure 3a). CX-1 cultures transduced with LV shNg-1 (shRNA to *NANOG*) were smaller than

those transduced with shNEG, the negative control vector, but not as small as cells transduced with shNp8-1 (Figure 3a). Similar results were obtained with LS 174T and Clone A cells were also sensitive to shNG-1 (Figure 3a). To insure that the inhibition of *NANOG* or *NANOGP8* was essential for this effect we also overexpressed the NANOG and NANOGP8 proteins and, as expected, found that such overexpression enhanced the growth of Clone A and CX-1 in suspension culture (Figure 3a). These data suggest that manipulation of the expression of NANOGP8 or NANOG directly affects 3-D growth.

LV shRNA Treatment in 3-D Culture Inhibits Subsequent Colony Formation

We next tested whether LV shRNA would continue to inhibit growth in those cells that survived the initial 72 hr exposure. CX-1 and Clone A spheroids and aggregates were recovered at the end of the assay, dissociated and replated in monolayer with complete medium. CX-1 and Clone A cells transduced with shNp8-1 had a ~30% significant decrease in regrowth in a colony formation assay (Figure 3 b, c). Transduction in 3-D culture had a longer growth inhibition than just the 3 days of the original suspension culture assay.

LV shRNA Transduction in 3-D Culture Does not Inhibit DNA Synthesis

We (17) and others (30-32) have shown that NANOG expression is associated with proliferation while inhibition of *NANOGs* decreases proliferation. We first tested whether CRC cells expressed the GFP reporter in suspension transduced with LV shRNA at low MOI. CX-1 spheroids transduced with LV shNp8-1 express the GFP reporter (Figure 4a) that can be localized to cells within a spheroid (Figures 4b-d). Analysis of GFP expression within the CRC cells in suspension culture transduced at MOI of 5 – 10 reveals that transduction occurred at an average of ~50% in Clone A, 60% in CX-1 and 67% in LS 174T (Panel e). Thus, roughly half of the CRC cells in suspension culture are transduced.

Then we asked whether cells transduced with LV shRNA were proliferating more slowly than cells that were not transduced using the EdU DNA synthesis method. DNA labeling of Clone A and CX-1 cells transduced with LV shRNAs had a minor (~ <10%) decrease in the percentage of all cells labeled with EdU (Figure 5, Panels a and c). However, there was no decrease in the percentage of cells labeled with EdU among the cells transduced with LV shNG-

1 or shNp8-1 compared to the labeling of cells transduced with LV shNEG (Figure 5c, d). Thus, inhibition of tumor growth in 3-D does not appear to be caused by inhibition of proliferation.

LV shRNA Increases Apoptosis in Suspension Cultures

We then questioned whether LV delivered shRNA to *NANOG* or *NANOGP8* in suspension cultures induced the expression of Annexin V and activation of caspases. CRC cells were cultured in SFM in suspension and transduced 24 hr later with LV shNG-1, shNp8-1 or shNEG or left Untreated. Expression of Annexin V in cells in suspension was compared to that in monolayer for CX-1 (Figure 6 e), Clone A (Figure 6 g) and LS 174T (Figure 6 i) as well as to the LV shNEG treated suspension culture controls for each cell line. LV transduced shNp8-1 significantly increased Annexin V expression in all 3 CRC lines compared to the LV shNEG control for each cell line (Figure 6 e, g, i). LV shNG-1 also increased Annexin V expression in Clone A (Figure 6g) and LS 174T (Figure 6i). Thus, LV delivered shRNA to *NANOGP8* and *NANOG* increased the cell death that occurs with suspension culture.

Since Laguinge et al (16) demonstrated that anoikis is caused by activation of caspase 8 in our cell lines, we then determined whether LV shNp8-1 or shNG-1 affected either caspase 8 or 9 activity in suspension culture. Single cell profiling was performed for caspase 3, 8 and 9 activity for cells cultured transduced with LV shRNA either in monolayer or suspension. shNp8-1 significantly increased the percentage of cells with active caspase 3 and 9 by 15% to 40% in all 3 cell lines compared to cells transduced with the shNEG control (Figure 6f, h, j). shNG-1 transduction did not increase the percentage of cells with active caspase 3 as often but did activate caspase 9 in all cell lines. shNp8-1 and shNG-1 had variable effects on the number of cells with caspase 8 activity. Thus, LV shRNA to *NANOGP8* and, to a lesser extent, *NANOG* increase caspase 3 activity with consistent increases in caspase 9 activity as the potential driver for anoikis through the intrinsic apoptotic pathway.

Inhibition of Caspase 3 and 9 Activity Blocks shNp8-1- and shNG-1-mediated Anoikis

To confirm the role of caspase activity, we inhibited the activity of caspases 3, 8, or 9 with peptidomimetics to block the ability of shRNA to either *NANOG* or *NANOGP8* to inhibit CRC growth in suspension. Transduction of the 3 cell lines with LV shNG-1 or shNp8-1 inhibited growth of the 3 CRC lines compared to the shNEG control by 20 – 50% in these

experiments (Figure 7a). When CRC in SFM suspension culture were exposed to 10 μM of cell permeant peptides for caspase 3 (Z-DEVD-FMK), caspase 8 (Z-IETD-FMK) or caspase 9 (Z-LEHD-FMK) 2 hr after LV transduction, inhibition of caspase 3 or 9 significantly stimulated growth in suspension in all 3 CRC lines transduced with shNp8-1 by 1.2- to 4-fold (Figure 7b-d). The caspase 8 inhibitor also blocked cell death in Clone A and CX-1 cells transduced with either shNp8-1 or shNG-1 (Figure 7c). Thus, transduction with LV shNp8-1 and to a lesser extent shNG-1 stimulated cell death through the intrinsic apoptotic pathway in all three CRC lines and through the extrinsic pathway in two.

Discussion

Anoikis was originally coined by Frisch and Francis (14) and has come to mean death by detachment or loss of integrin-mediated survival signals by loss of attachment to matrix or stroma. Vachon (33) has provided an excellent review in which anoikis is primarily initiated through activation of caspase 8 that directly activates the executioner caspases-3, -6, -7 that then initiate the programmed cell death sequence. However, other pathways also reinforce the cell death program that comes from cell detachment, namely the action of Death Associated Protein Kinase-1 (*DAPK1*) and Apoptosis Signaling Kinase-1 (*ASK1*) and survival also requires upregulation of survival factors that block anoikis. The present data suggest that the inhibition of either *NANOGP8* or *NANOG* activates the intrinsic pathway of apoptosis in cells exposed to anoikis.

Although three-dimensional growth affects a number of cell structure functions and protein expression, our data suggest that lentiviral transduction occurs in aggregates and spheroids even at MOIs of 5-10. The ligand for VSV-G protein that prseudotypes the LV is not well understood but may involve phosphatidyl serine on the inner aspect of the phospholipid membrane. As reviewed by Sun et al (34), phosphatidyl serine may bind VSV-G at low pH or by complexing with an as yet undefined protein that enhances lentiviral binding during membrane fusion. In either case our data indicate that transduction of 3-D structures occurs i*n vitro* and might be used to model interactions that occur in the tumor microenvironment *in vivo*.

Our data suggest that NANOGP8 and NANOG are anti-apoptotic proteins since inhibition of either *NANOG* family member increases anoikis in a caspase-dependent manner as measured by Annexin V binding (Figure 5e, g, i). We (17) had earlier shown that overexpression of *NANOGP8* or *NANOG* enhanced the ability of single CRC cells to survive and form spheroids and that as CRC cells survive in suspension culture the total expression of the *NANOG*s increases. This is important during embryonic development since there needs to be controlled proliferation and apoptosis. It may well be that the *NANOG*s role in carcinogenesis is not only to promote dedifferentiation and pluripotency but also to contribute to the resistance to treatments that induce apoptosis, such as chemotherapy (35, 36) and radiation therapy (37).

Clearly, expression of *NANOG* alone or with the other embryonic transcription factors *SOX2* and/or *OCT4* are also associated with resistance to chemotherapy (30, 38-40-29-32). We (17) have shown that inhibition of *NANOGP8* decreases the expression of *SOX2* and *OCT4* as have Siu et al. (41) reported that NANOG overexpression inhibits apoptosis. Noh et al (18) recently demonstrated that inhibition of the *NANOGs* inhibits MCL-1 expression through modulation of AKT activity. Our data support that conclusion and indicate that inhibition of the *NANOGs* may enhance the activity of BH3 peptides that block the pro-survival activity of the BCL-2 (BCL2) and BCL-xL (BCL2L1) prosurvival proteins (Mattoo et al, manuscript submitted[1]). Thus, in addition to its function in enhancing proliferation, NANOGP8 and NANOG have a prosurvival function that decreases caspase-dependent apoptosis, perhaps through AKT activation and increase in MCL-1 expression (19).

Laguinge et al (16) demonstrated that the extrinsic pathway of apoptosis was important for anoikis with its dependence on activation of caspase 8. In the present data caspase 9 activation appears more important because its inhibition led to consistent increases in growth in 3-D suspension cultures when either *NANOGP8* or *NANOG* was inhibited. The importance of this context is critical because the total level of *NANOG*-related transcripts increases in 3-D spheroids and the majority of this increase in transcripts is in *NANOGP8* expression (17). Thus, inhibition of the *NANOGs* may enhance the efficacy of therapy, especially if that treatment stimulates the expression of *NANOGs* as occurs during growth in suspension.

Our data support a role for either *NANOGP8* or *NANOG* in the regulation of caspase-dependent apoptosis in 3-D culture. The ability of shRNA to the *NANOGs* to induce apoptosis in monolayer as measured by Annexin V binding is quite low (Figure 5), presumably because the relative expression of the *NANOGs* is low (17). LV shNp8-1 generally had a greater inhibitory effect than shNG-1, but both were active. Since both shRNAs were identical except for the one nucleotide targeting base 759 in the coding sequence of NANOG and NANOGP8, the allelotypic inhibition is likely to reflect the greater presence of *NANOGP8* transcripts in CRC than *NANOG* transcripts. *NANOGP8* is expressed to a greater extent than *NANOG* in both CRC and liver metastases (17), but *NANOG* transcripts are also usually present in these CRC. *In silico* analysis

[1] Mattoo AR, Jingyu Zhang J, Luis A. Espinoza LA, Jessup JM. Inhibition of NANOG/NANOGP8 results in MCL-1 down regulation in colorectal cancer cells to enhance the therapeutic efficacy of BH3 mimetics. Submitted

of the proximal 2.5 Kb of the promoters for *NANOG* and *NANOGP8* suggest that while the promoters only share 40% homology there is similarity in the profile of binding of transcription factors predicted by the PhysBinder Transcription Factor binding program (42, 43). The only factors whose binding may be different are *STAT3, RAD21, NRF1, GABPA, ETS1* and *EGR1* in *NANOGP8* and *ESRRA, GATA1, JUNB, MAFK, SP1,* and *SP2* in *NANOG* (Supplemental Figure 3, Supplemental Table 1). Thus, both *NANOGs* may be activated, especially *NANOGP8* in the presence of inflammatory signals generated by stroma that activate the JAK/STAT (44, 45) and NF-kB (46, 47) pathways.

In summary, LV shRNA directed to *NANOGP8* or *NANOG* increases caspase 3 activity primarily through the intrinsic pathway of apoptosis in CRC cells exposed in 3-D growth to anoikis, an apoptotic stimulus. Our results support inhibition of *NANOGP8* and/or *NANOG* to increase the efficacy of clinical treatments that cause caspase-dependent apoptosis.

Acknowlegments: We thank Dr. Snorri S. Thorgeirsson for his support and helpful advice about this research. We also acknowledge the valuable advice and support of Drs Elizabeth Conner and Valentina Factor as well as the outstanding support of the Geneva Foundation, Tacoma, WA. Also, we gratefully acknowledge the support provided by the Center for Cancer Research of the NCI for Project ZIA BC 011199 and by the Department of Defense for Grant Number W81XWH-11-1-0327. The opinions expressed in this manuscript are those of the authors and do not necessarily represent those of the National Cancer Institute, the National Institutes of Health, the Department of Health and Human Services or the Department of the Army.

References

1. Lee GY, Kenny PA, Lee EH, Bissell MJ. Three-dimensional culture models of normal and malignant breast epithelial cells. Nat Methods 2007;4:359-65.
2. Fischbach C, Chen R, Matsumoto T, Schmelzle T, Brugge JS, Polverini PJ, et al. Engineering tumors with 3D scaffolds. Nat Methods. 2007;4:855-60.
3. Yamada KM, Cukierman E. Modeling tissue morphogenesis and cancer in 3D. Cell 2007;130:601-10.
4. Singh SK, Clarke ID, Terasaki M, Bonn VE, Hawkins C, Squire J, et al. Identification of a cancer stem cell in human brain tumors. Cancer Res 2003;63:5821-8.
5. Ponti D, Costa A, Zaffaroni N, Pratesi G, Petrangolini G, Coradini D, et al. Isolation and in vitro propagation of tumorigenic breast cancer cells with stem/progenitor cell properties. Cancer Res 2005;65:5506-11.
6. Charafe-Jauffret E, Ginestier C, Iovino F, Wicinski J, Cervera N, Finetti P, et al. Breast cancer cell lines contain functional cancer stem cells with metastatic capacity and a distinct molecular signature. Cancer Res 2009;69:1302-13.
7. Sato T, Stange DE, Ferrante M, Vries RG, Van Es JH, Van den Brink S, et al. Long-term expansion of epithelial organoids from human colon, adenoma, adenocarcinoma, and Barrett's epithelium. Gastroenterology 2011;141:1762-72.
8. St Croix B, Florenes VA, Rak JW, Flanagan M, Bhattacharya N, Slingerland JM, et al. Impact of the cyclin-dependent kinase inhibitor p27Kip1 on resistance of tumor cells to anticancer agents. Nat Med 1996;2:1204-10.
9. Francia G, Green SK, Bocci G, Man S, Emmenegger U, Ebos JM, et al. Down-regulation of DNA mismatch repair proteins in human and murine tumor spheroids: implications for multicellular resistance to alkylating agents. Mol Cancer Ther 2005;4:1484-94.
10. Håkanson M, Kobel S, Lutolf MP, Textor M, Cukierman E, Charnley M. Controlled breast cancer microarrays for the deconvolution of cellular multilayering and density effects upon drug responses. PLoS One 2012;7:e40141.

11. Li X, Zhang X, Zhao S, Wang J, Liu G, Du Y. Micro-scaffold array chip for upgrading cell-based high-throughput drug testing to 3D using benchtop equipment. Lab Chip 2013 Nov 28. [Epub ahead of print]
12. Longati P, Jia X, Eimer J, Wagman A, Witt MR, Rehnmark S, et al. 3D pancreatic carcinoma spheroids induce a matrix-rich, chemoresistant phenotype offering a better model for drug testing. BMC Cancer 2013 Feb 27;13:95.
13. Lee JM, Mhawech-Fauceglia P, Lee N, Parsanian LC, Lin YG, Gayther SA, et al. A three-dimensional microenvironment alters protein expression and chemosensitivity of epithelial ovarian cancer cells in vitro. Lab Invest 2013;93:528-42.
14. Frisch SM, Schaller M, Cieply B Mechanisms that link the oncogenic epithelial-mesenchymal transition to suppression of anoikis. J Cell Sci 2013;126(Pt 1):21-9.
15. Frisch SM, Francis H. Disruption of epithelial cell-matrix interactions induces apoptosis. J Cell Biol 1994;124:619-26.
16. Laguinge LM, Samara RN, Wang W, El-Deiry WS, Corner G, Augenlicht L, et al. DR5 receptor mediates anoikis in human colorectal carcinoma cell lines. Cancer Res 2008;68:909-17.
17. Zhang J, Espinoza LA, Kinders RJ, Lawrence SM, Pfister TD, Zhou M, et al. Nanog modulates stemness in human colorectal cancer. Oncogene 2013;32:4397-405.
18. Jeter CR, Badeaux M, Choy G, Chandra D, Patrawala L, Liu C *et al*. Functional evidence that the self-renewal gene NANOG regulates human tumor development. Stem Cells 2009;2**7**: 993-1005.
19. Noh KH, Kim BW, Song KH, Cho H, Lee YH, Kim JH, et a*l.* Nanog signaling in cancer promotes stem-like phenotype and immune evasion. J Clin Invest 2012;122**:** 4077-4093.
20. Mitsui K, Tokuzawa Y, Itoh H, Segawa K, Murakami M, Takahashi K, et al. The homeoprotein Nanog is required for maintenance of pluripotency in mouse epiblast and ES cells. Cell 2003;113:631-42.
21. Yamaguchi S, Kurimoto K, Yabuta Y, Sasaki H, Nakatsuji N, Saitou M, et al. Conditional knockdown of Nanog induces apoptotic cell death in mouse migrating primordial germ cells. Development. 2009;136:4011-20.

22. Guo Y, Mantel C, Hromas R A, Broxmeyer H E. Oct-4 Is Critical for Survival/Antiapoptosis of Murine Embryonic Stem Cells Subjected to Stress: Effects Associated with Stat3/Survivin. Stem Cells 2008;26:30-31.
23. Booth HA, Holland PW. Eleven daughters of NANOG. Genomics. 2004;84:229-38.
24. Fairbanks DJ, Fairbanks AD, Ogden TH, Parker GJ, Maughan PJ. NANOGP8: evolution of a human-specific retro-oncogene. G3 (Bethesda). 2012;2:1447-57.
25. Leith JT, Dexter DL, DeWyngaert JK, Zeman EM, Chu MY, Calabresi P, et al. Differential responses to x-irradiation of subpopulations of two heterogeneous human carcinomas in vitro. Cancer Res 1982;42:2556-61.
26. Weiss MJ, Wong JR, Ha CS, Bleday R, Salem RR, Steele GD Jr, et al. Dequalinium, a topical antimicrobial agent, displays anticarcinoma activity based on selective mitochondrial accumulation. Proc Natl Acad Sci U S A. 1987;84:5444-8.
27. Tom BH, Rutzky LP, Oyasu R, Tomita JT, Goldenberg DM, Kahan BD. Human colon adenocarcinoma cells. II. Tumorigenic and organoid expression in vivo and in vitro. J Natl Cancer Inst 1977;58:1507-12.
28. Niles RM, Wilhelm SA, Steele GD Jr, Burke B, Christensen T, Dexter D, et al. Isolation and characterization of an undifferentiated human colon carcinoma cell line (MIP-101). Cancer Invest 1987;5:545-52.
29. Morikawa K, Walker SM, Jessup JM, Fidler IJ. In vivo selection of highly metastatic cells from surgical specimens of different primary human colon carcinomas implanted into nude mice. Cancer Res 1988;48:1943-8.
30. Jeter CR, Liu B, Liu X, Chen X, Liu C, Calhoun-Davis T, et al. NANOG promotes cancer stem cell characteristics and prostate cancer resistance to androgen deprivation. Oncogene 2011;30:3833-45.
31. Uchino K, Hirano G, Hirahashi M, Isobe T, Shirakawa T, Kusaba H et al. Human Nanog pseudogene8 promotes the proliferation of gastrointestinal cancer cells. Exp Cell Res. 2012;318:1799-807.
32. Ishiguro T, Sato A, Ohata H, Sakai H, Nakagama H, Okamoto K. Differential expression of nanog1 and nanogp8 in colon cancer cells. Biochem Biophys Res Commun. 2012;418:199-204.

33. Vachon PH. Integrin signaling, cell survival, and anoikis: distinctions, differences, and differentiation. J Signal Transduct 2011;2011:738137.
34. Sun X, Roth SL, Bialecki MA, Whittaker GR. Internalization and fusion mechanism of vesicular stomatitis virus and related rhabdoviruses. Future Virol 2010;5:85-96.
35. Eischen CM, Kottke TJ, Martins LM, Basi GS, Tung JS, Earnshaw WC, et al. Comparison of apoptosis in wild-type and Fas-resistant cells: chemotherapy-induced apoptosis is not dependent on Fas/Fas ligand interactions. Blood 1997;90:935-43.
36. Tomicic MT, Christmann M, Kaina B. Topotecan triggers apoptosis in p53-deficient cells by forcing degradation of XIAP and survivin thereby activating caspase-3-mediated Bid cleavage. J Pharmacol Exp Ther 2010;332:316-25.
37. Lawrence TS, Davis MA, Hough A, Rehemtulla A. The role of apoptosis in 2',2'-difluoro-2'-deoxycytidine (gemcitabine)-mediated radiosensitization. Clin Cancer Res. 2001;7:314-9.
38. Zhang Z, Zhu Y, Lai Y, Wu X, Feng Z, Yu Y, et l. Follicle-stimulating hormone inhibits apoptosis in ovarian cancer cells by regulating the OCT4 stem cell signaling pathway. Int J Oncol 2013;43:1194-204.
39. Yang L, Zhang X, Zhang M, Zhang J, Sheng Y, Sun X, et al. Increased Nanog expression promotes tumor development and Cisplatin resistance in human esophageal cancer cells. Cell Physiol Biochem 2012;30:943-52.
40. Latifi A, Abubaker K, Castrechini N, Ward AC, Liongue C, Dobill F, et al. Cisplatin treatment of primary and metastatic epithelial ovarian carcinomas generates residual cells with mesenchymal stem cell-like profile. J Cell Biochem 2011;112:2850-64.
41. Siu MK, Wong ES, Chan HY, Ngan HY, Chan KY, Cheung AN. Overexpression of NANOG in gestational trophoblastic diseases: effect on apoptosis, cell invasion, and clinical outcome. Am J Pathol 2008;173:1165-72.
42. Hooghe B, Broos S, van Roy F, De Bleser P. A flexible integrative approach based on random forest improves prediction of transcription factor binding sites. Nucleic Acids Res. 2012;40:e106.
43. Broos S, Soete A, Hooghe B, Moran R, van Roy F, De Bleser P. PhysBinder: improving the prediction of transcription factor binding sites by flexible inclusion of biophysical properties. Nucleic Acids Res 2013;41:W531-4.

44. Lieblein JC, Ball S, Hutzen B, Sasser AK, Lin HJ, Huang TH, et al J. STAT3 can be activated through paracrine signaling in breast epithelial cells. BMC Cancer 2008;8:302.
45. Calon A, Espinet E, Palomo-Ponce S, Tauriello DV, Iglesias M, Céspedes MV, et al. Dependency of colorectal cancer on a TGF-β-driven program in stromal cells for metastasis initiation. Cancer Cell 2012;22:571-84.
46. Yeung TL, Leung CS, Wong KK, Samimi G, Thompson MS, Liu J, et al. TGF-β modulates ovarian cancer invasion by upregulating CAF-derived versican in the tumor microenvironment. Cancer Res 2013;73:5016-28.
47. Erez N, Glanz S, Raz Y, Avivi C, Barshack I. Cancer associated fibroblasts express pro-inflammatory factors in human breast and ovarian tumors. Biochem Biophys Res Commun. 2013;437:397-402.

FIGURE LEGENDS

Figure 1. Lentiviral shRNA to the NANOGs Inhibits Tumor Growth and Expression of the *NANOGs*. Panel a – CX-1 tumors in NOD/SCID mice were injected injected with LV shNG-1 (Open Circles) or shNp8-1 (Closed circles) for the combined *NANOG* shRNAs or with shNEG (Open Triangles) or Uninjected (Solid Squares) for the Controls. Tumor areas were calculated as described in the Methods and then the Tumor Areas before intralesional injection subtracted from the area 8 days later (D8-D0 Tumor Area in mm^2). The tumors injected with LV shRNA to either *NANOG* or *NANOGP8* were significantly smaller than the Controls (P=0.03). Fluorescence imaging of monolayer and suspension cultures was performed as described in Supplementary Figure 1 for NANOG expression **(Panel b)** and TUNEL **(Panel c)**. The % of cells positive for NANOG or TUNEL in monolayer and spheroid cultures are presented as mean ± SD. † is P< 0.0001 of spheroid versus monolayer values. Clone A **(Panel d)**, CX-1 **(Panel e)** or LS 174T **(Panel f)** were cultured in suspension for 16 hours and then transduced with a control lentivirus (LV shNEG), or lentivirus with shRNA to *NANOG* (shNG-1) or *NANOGP8* (shNp8-1) at a MOI of 5-10 and cultured for a subsequent 56 hr. Cells were collected and RNA extracted with qRT-PCR performed for total *NANOG*-related transcripts. Results are the mean ± SD of the Ct of NANOG transcripts normalized by the expression of the housekeeping gene GAPDH and expressed as the % of the Control untreated CRC cells as performed in (19). P values determined by one way ANOVA with Holm-Sidak test for means **(Panels c-e)**.

Figure 2. Effect of LV delivered shRNA on CRC in Suspension Culture. **(Panel a)** Schema for suspension experiments where 2,000 CRC cells transfected with *Luc2* are cultured in SFM in ULLA 96 well microtiter plates in triplicate. A day later CRC were transduced with LV shRNAs at MOI of 5 -10 and then 3 days later individual wells were imaged on an inverted epi-fluorescent inverted microscope. **(Panel b)** Typical images of CX-1 cells treated as described in Panel a. **(Panel c)** The area of the CX-1 cultures in Panel B were measured in ImageJ and results presented in mean arbitrary units (AU) ± SD.

(Panel d) Well contents were aspirated, transferred to luminescent 96 well plates and luminescence measured. Values are Mean Luminescence ± SD of the cultures in Panel b. Correlation between values for Tumor Area and Luminescence were converted to % of the untreated control cultures and then analyzed by simple regression. The Correlation between Luminescence and Tumor Area for CX-1 **(Panel e)** and Clone A **(Panel f)** are presented with at least 3 independent experiments for each cell line.

Figure 3. Effect of Inhibition of NANOG or NANOGP8 on Growth in Suspension Culture. (Panel a) CRC cell lines were treated with LV-delivered shRNA as described in Figure 2 or transduced with LV-delivered NANOG or NANOGP8 to overexpress the respective protein. Tumor Area was then imaged as described in Figure 2 and the results of at least 3 independent experiments for each of the cell lines are presented in terms of the Mean ± SD of the change in Tumor Area from the untreated control cells for each cell line. The P values are compared to the LV shNEG for each CRC cell line by one-way ANOVA with Holm-Sidak correction for multiple comparisons. The cells transduced with LV shNp8-1 were each significantly smaller at the $P< 0.01$ level against the respective shNEG control. Only Clone A and CX-1 were transduced to overexpress NANOG or NANOGP8 since LS 174T was more spherogenic than Clone A or CX-1. CX-1 **(Panel b)** and Clone A **(Panel c)** viable cells were collected at the end of the cultures and replated in complete medium in monolayer culture. Colonies were then identified at 2 weeks after staining with crystal violet and counted. Results are mean ± SD with P values determined by one-way ANOVA with Holm-Sidak corrections for multiple comparisons to LV shNEG.

Figure 4 Lentiviral Transduction Efficiency of CRC Spheroids. CX-1 spheroids were established and transduced with LV shNp8-1 as described in Figure 2 and imaged with confocal microscopy. Spheroids were imaged in planar sections in the fluorescein channel to detect GFP **(Panel a)**, DAPI-stained nuclei in the UV channel **(Panel b)**, transilluminated to assess cell location **(Panel c)**, and the merged image is presented in **(Panel d)** to assess transduction efficiency. The white bar in **(Panel c)** is 15 microns. The percentage of cells

within each plane of the confocal image that were GFP+/DAPI+ was analyzed for Clone A, CX-1, LS 174T where transduction was performed at MOI's of 5 -10 and results are presented as Mean ± SD of cells that are GFP+ in **(Panel e)**. Confocal sections were selected at least 20 microns apart to insure that cells were counted only once.

Figure 5. LV Treatment in 3-D Culture Does Not Decrease Proliferation. Clone A **(Panels and c)** and CX-1 **(Panels b and d)** cells were transduced with the indicated LV shRNA or left untreated as described for Figure 2. At 56 hr after transduction the CRC cells were labeled with EdU and then at 72 after transduction cells were harvested and processed for DNA labeling per the manufacturer's protocol. Total DNA labeling was measured (Panels a and b) with results expressed as the mean ± SD of % of cells that contained fluorescent label (% Proliferation). At least 500 cells per group were counted. P values determined by one-way ANOVA and compared to the untreated control (None) with Holm-Sidak correction for multiple comparisons. **Panels c and d** present the mean ± SD of % Proliferation for Clone A and CX-1 cells, respectively, that were transduced by LV and expressing GFP.

Figure 6. Single Cell Profiling of CRC for Caspase 3, 8 and 9 Activity and Annexin V Expression after LV shRNA treatment in Monolayer and Suspension Culture. (Panel a) LS 174T spheroids transduced with LV shNp8-1 as described in Figure 2 were incubated with 1 μM cell permeant caspase 3 substrate *DEVDGI* (PhiPhiLux G_2D_2, Oncoimmunin) for 45 min at 37°C and imaged for rhodamine fluorescence. The same spheroid was then imaged to detect GFP as a reporter for the LV transduction **(Panel b),** transilluminated for cell location **(Panel d)** with resultant merged image **(Panel c)**. White bar is 15 microns. Single cell profiling of annexin V expression **(Panels e, g, i)** and caspase activity **(Panels f, h, j)** was also performed by static cytometry. CX-1 **(Panels e, f)**, Clone A **(Panels g, h)** and LS 174T **(Panels i, j)** cells were cultured in monolayer and suspension culture and treated with LV shRNA as described in Figure 2. Annexin expression was measured by fluorescence in individual cells and results presented as mean ± SD % Annexin positive cells. † is $P < 0.001$ compared to LV shNEG by one- way ANOVA with Holm-Sidak correction

for multiple comparisons **(Panels e, g, i)**. Caspase activity was assessed in 3-D cultures in individual cells by incubation with the cell permeant fluorogenic peptide substrates for Caspases 3, 8 and 9 (Phiphilux, CaspaLux 8 L_2D_2 and CaspaLux M_2D_2, respectively, Oncoimmunin) according to the manufacturers instructions. Cells were untreated in monolayer ( ) or suspension ( ) or cultured in suspension and transduced with LV shNEG ( ), LV shNG-1 ( ) or LV shNp8-1 ( ). Results are the means ± SD of the percentage of cells that were caspase active and the P values compared to the suspension LV shNEG transduced cells within each caspase activity group. † is $P < 0.001$ compared to the LV shRNA control by two-way ANOVA with Holm-Sidak correction **(Panels f, h, j)**.

Figure 7. Caspase Inhibitors Block Anoikis and LV shRNA in 3-D Suspension Culture. (**Panel a**) The 3 CRC lines were transduced with LV shRNAs as described in Figure 1 without any caspase inhibitors. LV shNG-1 and shNp8-1 significantly inhibit the growth in suspension culture of all 3 cell lines. Results are mean ± SD of growth normalized by each CRC cells cultured in suspension in SFM. Black column represents CX-1, Light gray represents LS 174T and dark gray is Clone A. Π $P<0.01$ versus shNEG control for each cell line ; † $P< 0.001$ versus shNEG control for each cell line. **Panels b, c, d** represent results with CX-1, Clone A, and LS 174T, respectively. CRC cells are cultured in suspension in SFM and transduced with LV shRNA as described in Figure 2 and then incubated with 10 μM of a Caspase 3 (Z-DEVD-FMK), Caspase 8 (Z-IETD-FMK), or Caspase 9 (Z-LEHD-FMK) inhibitor. Cells were left Untreated ( ), transduced with LV shNEG ( ), transduced with shNG-1 ( ), or transduced with shNp8-1 ( ). Results are the mean ±SD of the area of tumor growth in each CRC line, LV treatment and caspase inhibitor group normalized against suspension cultures of the same CRC cell line and LV treatment in the absence of the caspase inhibitor. Two-way ANOVA was performed with Holm-Sidak correction for multiple comparisons. Π is $P<0.01$ and † is $P<0.001$ compared to cells cultured without the indicated caspase inhibitor, e.g. caspase 3 inhibitor-treated Clone A cells transduced with LV shNp8-1 in **panel c** occupy an area ~350% larger than the same cells transduced with LV shNp8-1 in the absence of the caspase 3 inhibitor

Supplemental Figures and Tables

Supplemental Figure 1. Suspension Culture Increases NANOG Protein and TUNEL Expression. CX-1 **(Panels A and B)** or KM-12c **(Panels C and D)** were cultured either in monolayer **(Panels A and C)** or in suspension culture **(Panels B and D)** for 72 hours and then stained for TUNEL positivity (Green) or NANOG (RED) with DAPI (Blue) to indicate the location of cell nuclei. The fluorescence images were collected in grayscale on an inverted epi-fluorescence microscope and then analyzed as described previously (16) with indirect immunofluorescence detecting NANOG instead of DR5.

Supplemental Figure 2. Predicted Transcription Factor Binding Sites in the Promoters of *NANOG* and *NANOGP8*. The proximal 2.5 Kb upstream of the Translation Start Site for each gene was analyzed with the Physbinder program (42, 43). The binding site for each of the Transcription Factors that are predicted to bind to the promoter are depicted with appropriate colors. The prediction probability for each factor was set by the average of the Positive Predictive Value and the F value with a threshold of greater than 500. † denotes predicted STAT3 binding sites. * denotes other transcription factors that are predicted to be differentially expressed between the two promoters.

Supplemental Table 1. Predicted Transcription Factor Binding Sites on the *NANOG* and *NANOGP8* 2.5 Kb promoters

A. Factors that Bind Both Promoters:

	Promoter (# of Sites)	
Gene	*NANOG*	*NANOGP8*
BRCA1	2	4
CTCF	1	4
CTCFL	1	1
FOS	3	2
GATA2	1	4
GTF3C2	5	3
IRF3	1	3
KFL4	17	16
MAFF	3	2
MEF2C	2	3
NANOG	2	1
POL3RA	2	2
POU5F1	4	1
RELA	30	26
RUNX3	5	7
SPI1	1	1
SREBF1	4	3
TCF12	2	3
YY1	1	4
ZEB1	3	5

B. Transcription Factors Predicted to Bind to One or Other Promoter

NANOG Specific		*NANOGP8* Specific	
Factor	# 0f Sites	Factor	# of Sites
ESRRA	4	EGR1	1
GATA1	2	ETS1	1
JunB	2	GABPA	3
MAFK	3	NRF1	1
SP1	2	RAD21	2
SP2	3	STAT3	2

Legend. The promoter sequences of both *NANOG* and *NANOGP8* 2.5 Kb upstream of the TSS were analyzed with the Physbinder program (42, 43) using the average binding model for human transcription factors. The data are presented in A for those factors that are predicted to bind both promoters whereas in B are listed the factors that are predicted to bind one or the other promoter. The number of individual binding sites for each factor are also presented (# of Sites).

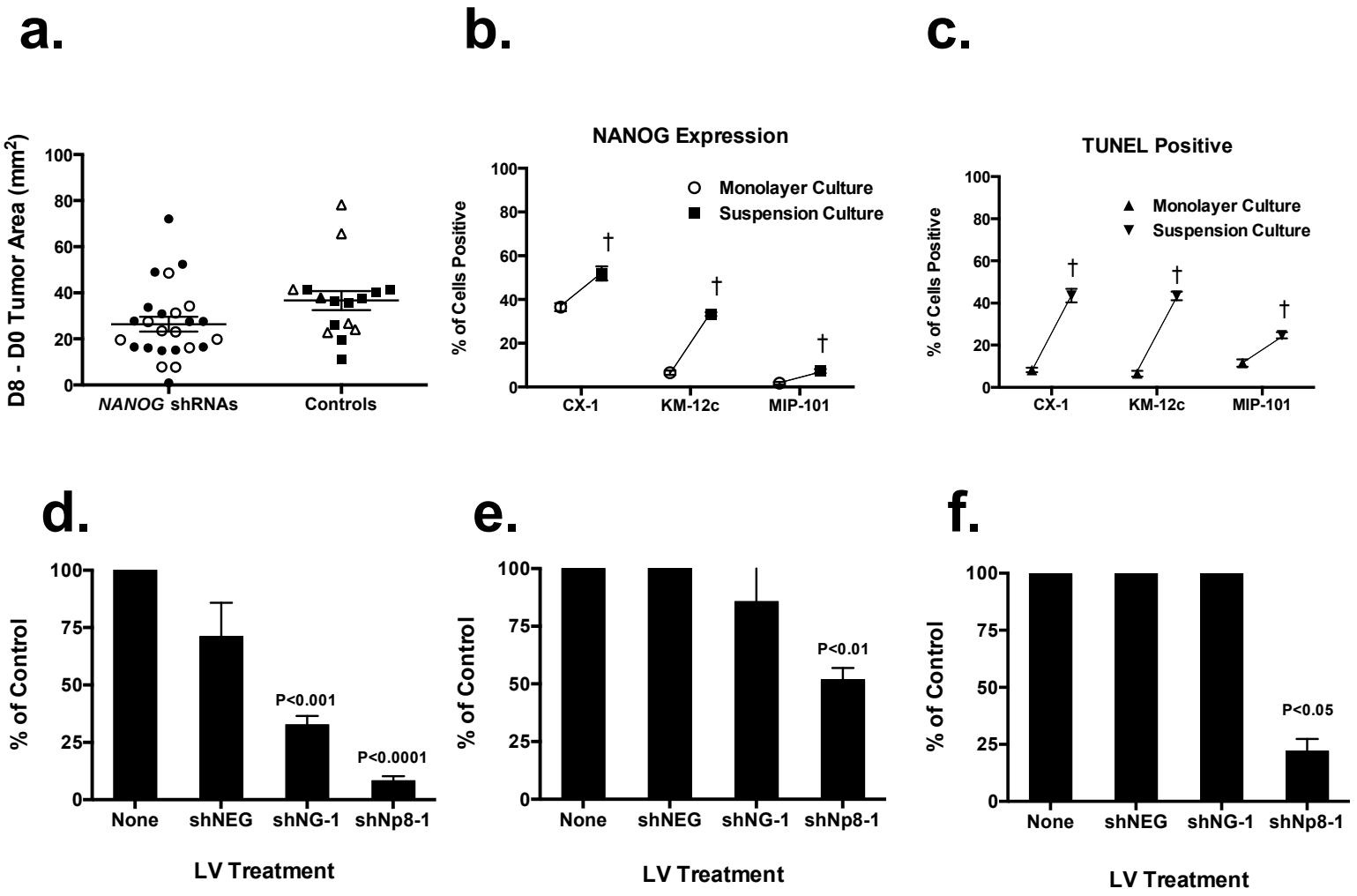
a.
b.
c.
D8 - D0 Tumor Area (mm2)
NANOG shRNAs
Controls
NANOG Expression
% of Cells Positive
Monolayer Culture
Suspension Culture
CX-1
KM-12c
MIP-101
TUNEL Positive
d.
e.
f.
% of Control
P<0.001
P<0.0001
P<0.01
P<0.05
None
shNEG
shNG-1
shNp8-1
LV Treatment

Figure 1

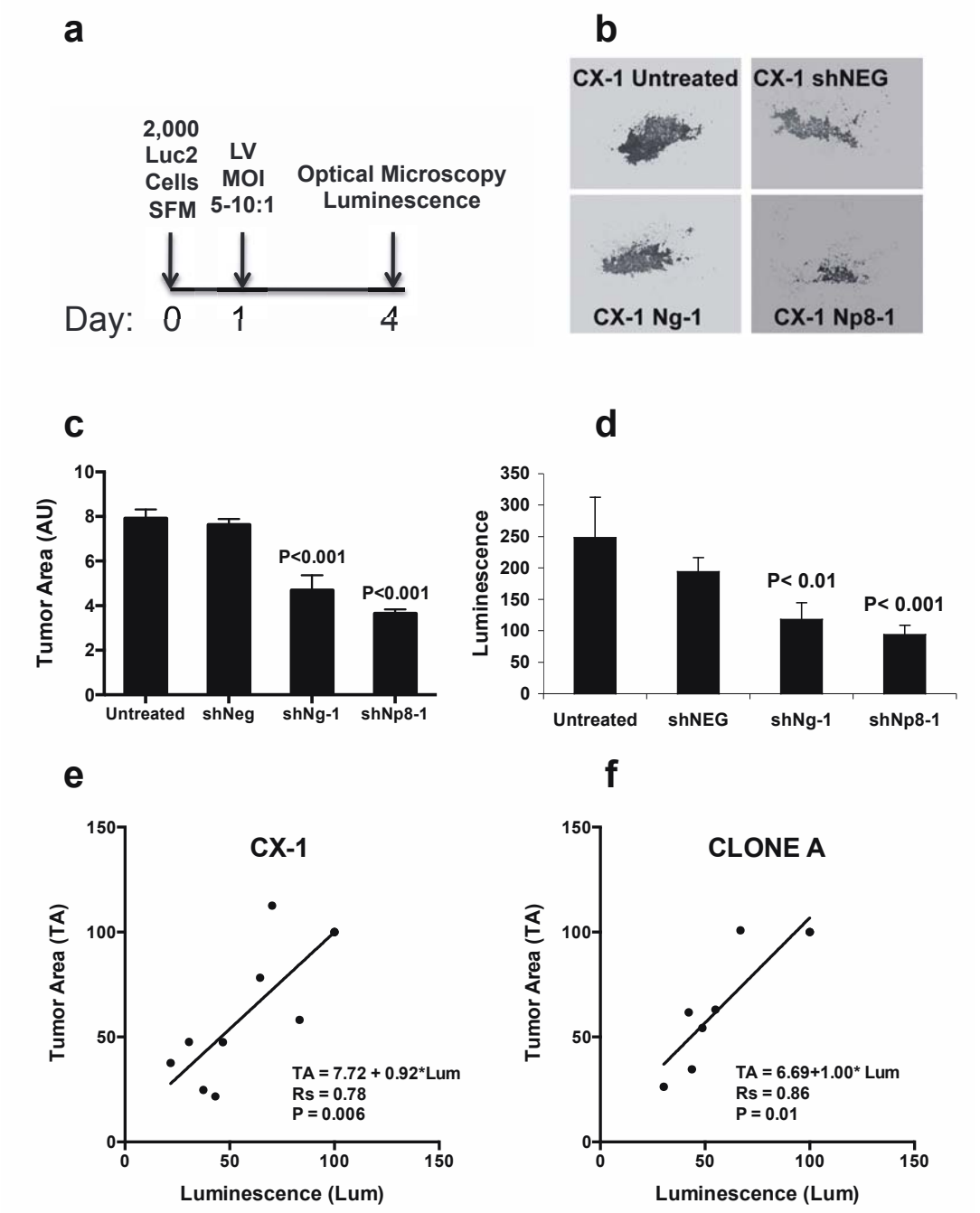
a
2,000 Luc2 Cells SFM
LV MOI 5-10:1
Optical Microscopy Luminescence
Day: 0 1 4
b
CX-1 Untreated
CX-1 shNEG
CX-1 Ng-1
CX-1 Np8-1
c
Tumor Area (AU)
P<0.001
P<0.001
Untreated
shNeg
shNg-1
shNp8-1
d
Luminescence
P< 0.01
P< 0.001
Untreated
shNEG
shNg-1
shNp8-1
e
CX-1
Tumor Area (TA)
TA = 7.72 + 0.92*Lum
Rs = 0.78
P = 0.006
Luminescence (Lum)
f
CLONE A
Tumor Area (TA)
TA = 6.69+1.00* Lum
Rs = 0.86
P = 0.01
Luminescence (Lum)

Figure 2

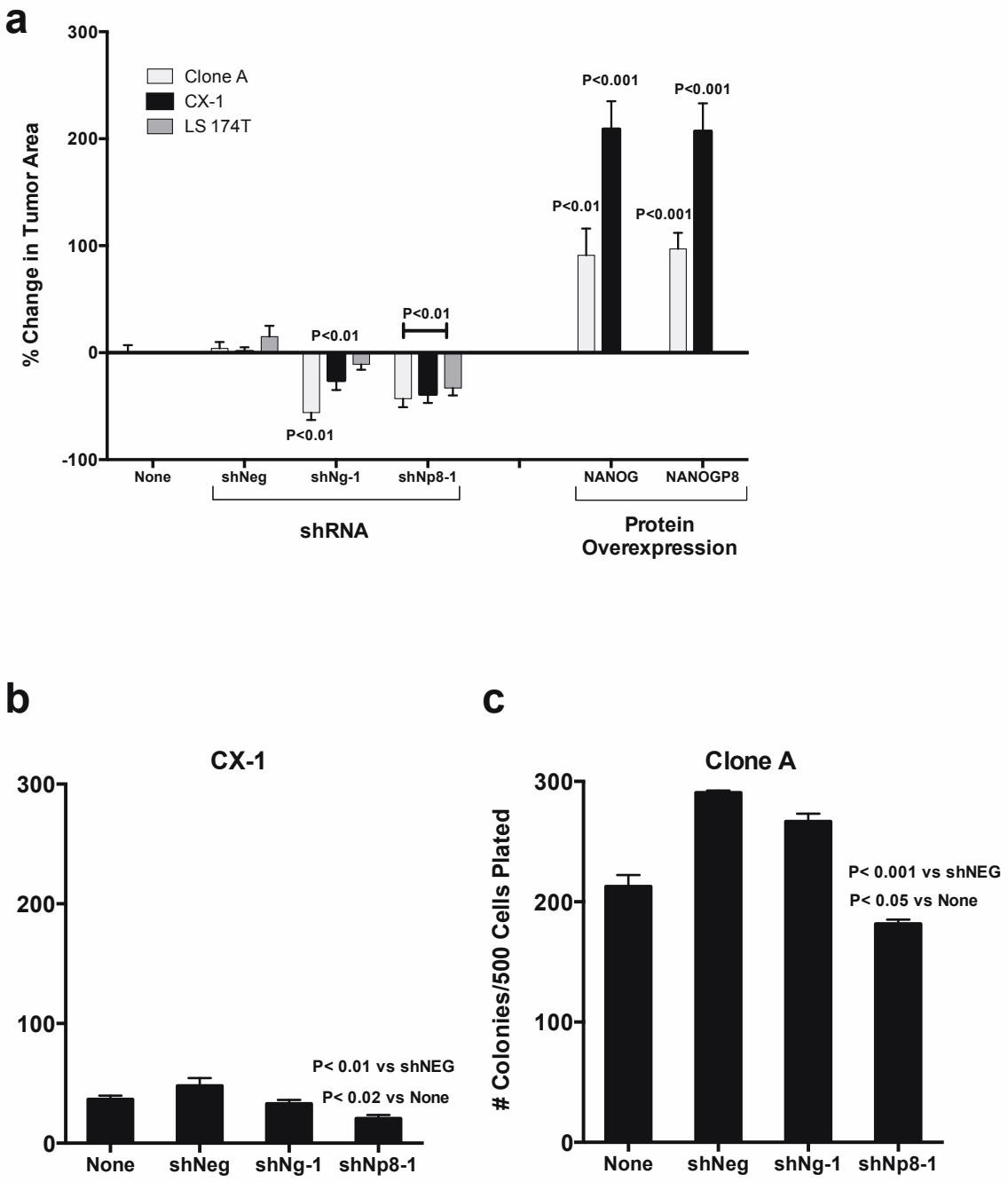
a
300
200
100
0
-100
% Change in Tumor Area
Clone A
CX-1
LS 174T
P<0.001
P<0.001
P<0.01
P<0.001
P<0.01
P<0.01
P<0.01
None
shNeg
shNg-1
shNp8-1
NANOG
NANOGP8
shRNA
Protein Overexpression
b
CX-1
Colonies/500 Cells Pated
300
200
100
0
P< 0.01 vs shNEG
P< 0.02 vs None
None
shNeg
shNg-1
shNp8-1
c
Clone A
Colonies/500 Cells Plated
300
200
100
0
P< 0.001 vs shNEG
P< 0.05 vs None
None
shNeg
shNg-1
shNp8-1

Figure 3

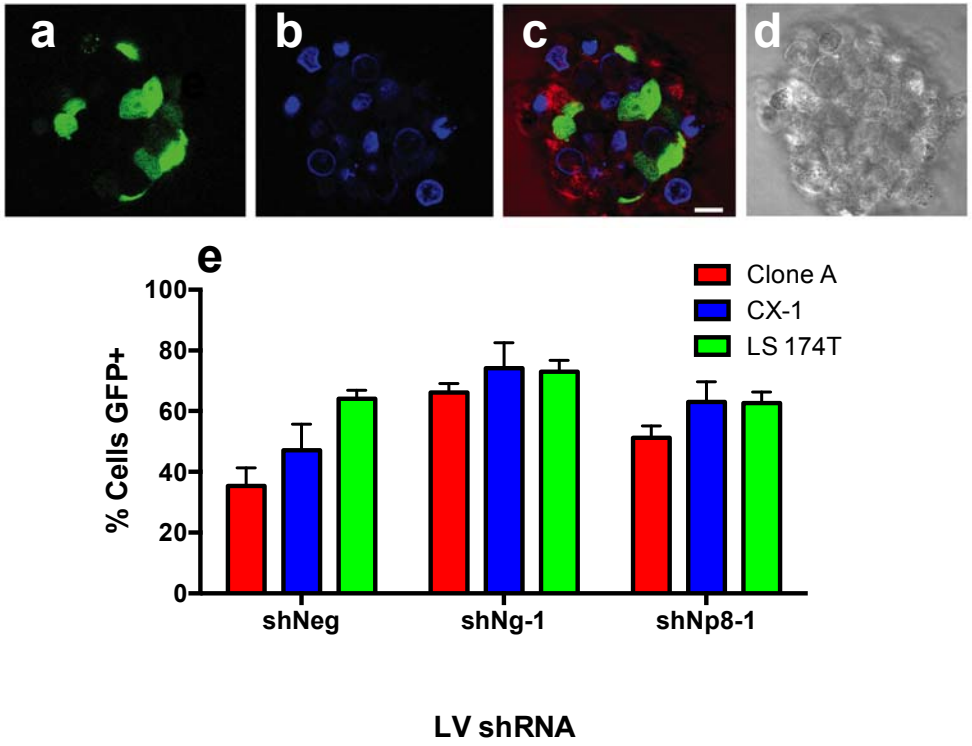
a
b
c
d
e
Clone A
CX-1
LS 174T
% Cells GFP+
100
80
60
40
20
0
shNeg
shNg-1
shNp8-1
LV shRNA

Figure 4

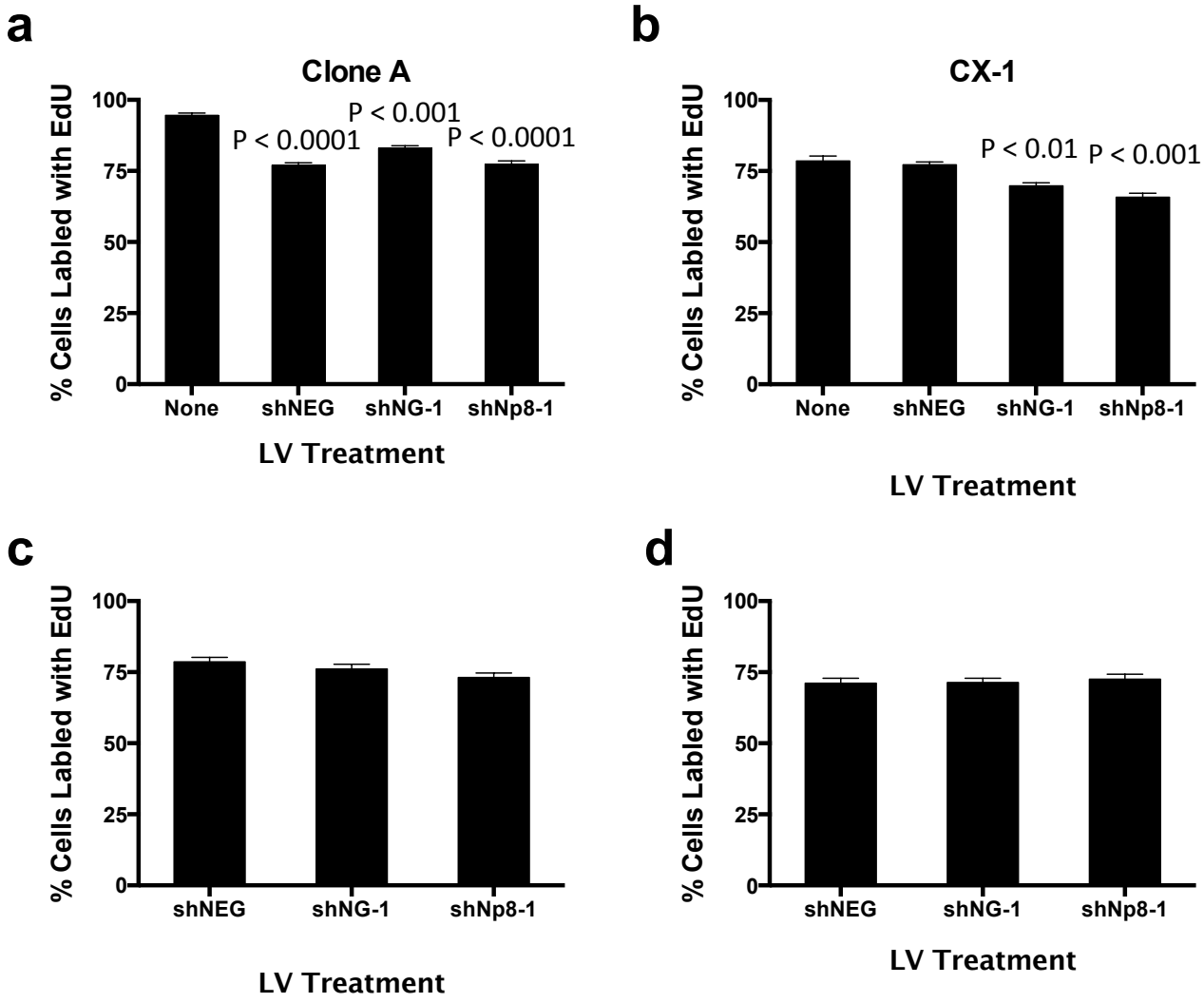
a
Clone A
% Cells Labled with EdU
100
75
50
25
0
P < 0.0001
P < 0.001
P < 0.0001
None
shNEG
shNG-1
shNp8-1
LV Treatment
b
CX-1
% Cells Labled with EdU
P < 0.01
P < 0.001
None
shNEG
shNG-1
shNp8-1
LV Treatment
c
% Cells Labled with EdU
shNEG
shNG-1
shNp8-1
LV Treatment
d
% Cells Labled with EdU
shNEG
shNG-1
shNp8-1
LV Treatment

Figure 5

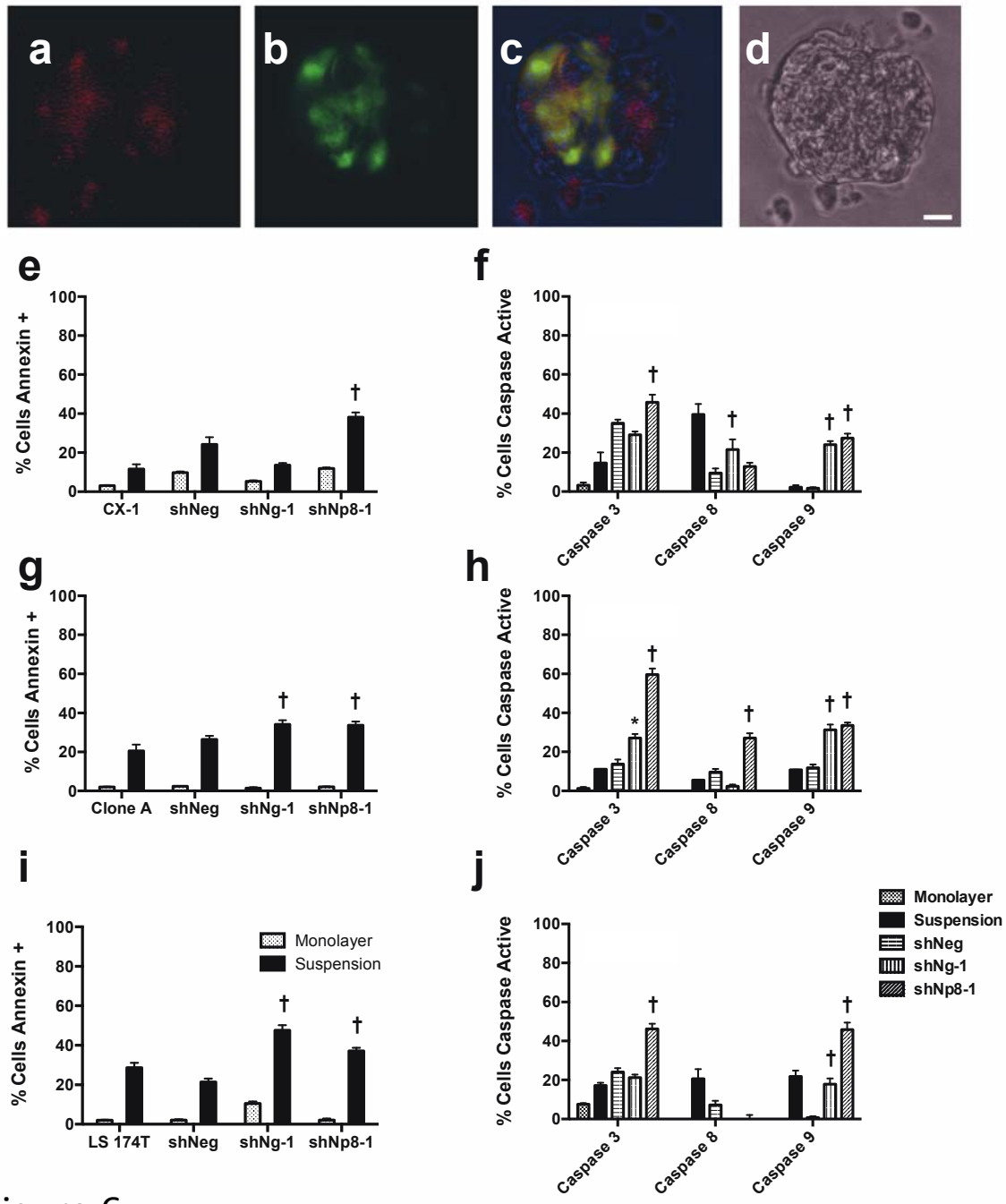
a
b
c
d
e
% Cells Annexin +
CX-1
shNeg
shNg-1
shNp8-1
f
% Cells Caspase Active
Caspase 3
Caspase 8
Caspase 9
g
Clone A
h
i
LS 174T
Monolayer
Suspension
j
shNeg
shNg-1
shNp8-1

Figure 6

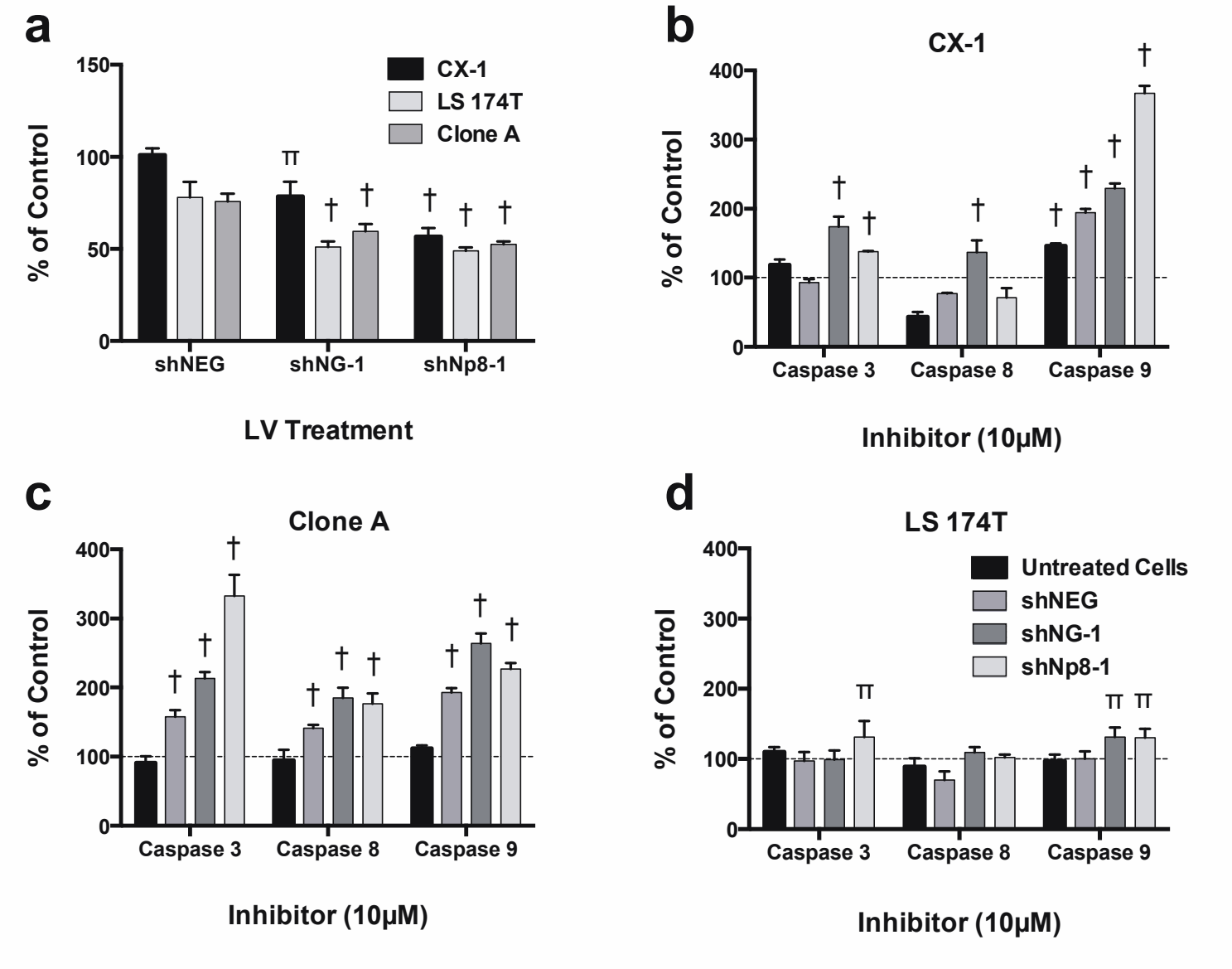
a
150
100
50
0
% of Control
CX-1
LS 174T
Clone A
π
†
shNEG
shNG-1
shNp8-1
LV Treatment
b
CX-1
400
300
200
100
0
% of Control
†
Caspase 3
Caspase 8
Caspase 9
Inhibitor (10μM)
c
Clone A
400
300
200
100
0
% of Control
†
Caspase 3
Caspase 8
Caspase 9
Inhibitor (10μM)
d
LS 174T
400
300
200
100
0
% of Control
Untreated Cells
shNEG
shNG-1
shNp8-1
π
Caspase 3
Caspase 8
Caspase 9
Inhibitor (10μM)

Figure 7